The Thermoelectric Properties of Boron-Doped Silicon and Silicon-Germanium in the as-Hot Pressed Condition

September 30, 1988

Prepared for:

United States Army
SLCET-PE
Fort Monmouth, New Jersey

Prepared by:

Cronin B. Vining
Jet Propulsion Laboratory/
California Institute of Technology
Pasadena, California 91109

ABSTRACT

The figure of merit has been determined for samples of silicon and silicon germanium with various amounts of boron doping. To date, samples have been characterized in the "as-hot-pressed" state in order to provide a basis for evaluating the effect of annealing on the thermoelectric properties. Thermoelectric properties have been determined up to 1300 K and microstructural examinations have been performed. As anticipated, figure of merit values are relatively low in the as-hot-pressed state, but homogenization by annealing (planned as a future activity) is expected to improve both the electrical and thermal properties. Notable are results for a boron-doped silicon sample which has a very large electrical power factor (up to 45 $\mu W/cm\text{-}K^2$) and reaches a maximum $ZT_{peak}=0.2$, much higher than might be expected without germanium alloying. Recommendations are made following the summary for future efforts in this area.

ACKNOWLEDGEMENTS

The work described in this paper was carried out at the Jet Propulsion Laboratory/California Institute of Technology and at Thermo Electron Corporation, under contract with the National Aeronautics and Space Administration with support from the United States Army, SLCET-PE, Fort Monmouth, New Jersey. Principle participants at JPL have been C. Vining, C. Wood, A. Zoltan and J. Parker. Principle participants at Thermo Electron have been V. Raag, M. Platek and R. Masters.

INTRODUCTION

This report summarizes the results of thermoelectric property measurements on ten samples of silicon and silicon-germanium prepared with and without boron doping. The goal of the program is first improve the understanding of p-type SiGe-based materials and ultimately develop p-type materials with significantly improved figure of merit values. The current phase of the program has emphasized characterization of samples in the as-hot pressed state to serve as a baseline for future heat treatment studies. The study of boron-doped silicon and silicon germanium has been motivated by several factors described below.

Significant improvements in thermoelectric figure of merit values have been reported to result from heat treatments of n-type silicon-germanium (SiGe) alloys doped with gallium phosphide (SiGe/GaP).[1,2] The potential for improvement, however, may be even larger for the p-type materials since the figure of merit of p-type SiGe-based materials is generally lower than n-type SiGe-based materials. Moreover, a device based upon a combination of the improved n-type SiGe/GaP materials and conventional (unimproved) p-type SiGe materials will realize only about 1/2 the performance improvement achieved in the n-type SiGe/GaP material alone. Thus, to achieve the maximum weight savings and power output gains for SiGe-based thermoelectric power systems, increasing attention should be focused on improving the performance of p-type materials.

Previous attempts to improve p-type SiGe by doping with both boron and GaP were frustrated by cross-doping effects.[3] The high solubility of phosphorus in silicon-germanium resulted in n-type materials in the as-hot pressed state, in spite of large excesses of the p-type dopant, boron.[4] Attempts to avoid the cross-doping effects by using other III-IV compounds have resulted in disappointingly low power factor (S^2/ρ) values to date. Recently it has been observed that samples doped with a large excess of boron (up to 20 atomic percent) have exhibited remarkably high power factor values. The present program has been designed to study this effect more closely and determine the potential for high figure of merit values in the silicon-rich region of the boron-silicon-germanium system.

EXPERIMENTAL DETAILS

Ten samples in the silicon-boron-germanium system were prepared with the compositions and hot pressing parameters listed in Table 1. In order to prepare the boron-doped silicon samples, a preliminary hot pressing of a large (1.5" diameter) compact of 80 a/o Si-20 a/o Ge (where a/o indicates atomic percent) was prepared by mixing -325 mesh powders of silicon and boron. This compact was then re-pulverized to -325 mesh and blended with -325 mesh silicon powder to prepare 0.5" diameter compacts of boron-doped silicon (samples T-467, T-464, T-479 and T-468). The remaining six compacts were prepared from blended stoichiometric mixtures of -325 mesh powders of the elements in a single hot pressing step.

Table 1: Summary of Compositions and Pressing Conditions

#	ID#	Si a/o	Ge a/o	B a/o	T °C	t hrs	Number of Pressings	Pressure KPSI	Density g/cm^3
1	T450	100			1250	2	1	28.8	2.304
2	T475	80	20		1150	2	1	28.8	2.884
3	T467	99.9		0.1	1250	2	2	28.8	2.315
4	T464	99		1	1250	2	2	28.8	2.330
5	T479	90		10	1173	2	2	31.7	2.284
6	T468	80		20	1250	2	2	28.8	2.355
7	T478	98	1	1	1175	2	1	31.7	2.335
8	T477	94	5	1	1150	2	1	28.8	2.445
9	T476	89	10	1	1150	2	1	28.8	2.611
10	T437	64	16	20	1175	4	1	26.6	2.829

The samples were examined using scanning electron microscopy, optical microscopy, and x-ray diffraction at Thermo Electron. These results are summarized in a separate report issued by Thermo Electron.[5] The electrical resistivity (ρ) and Seebeck coefficient (S) were determined from room temperature to 1000 °C and the density was also determined at Thermo Electron. At JPL, the electrical resistivity (ρ) and Hall coefficient (R_H) were determined from room temperature to 1000 °C and the thermal diffusivity and heat capacity were determined from 300 °C to 1000 °C, as was the density. From these measurements, values for the electrical power factor (S^2/ρ), Hall mobility (μ_H), thermal conductivity (λ), figure of merit ($Z=S^2/\rho\lambda$) and dimensionless figure of merit ($ZT=S^2T/\rho\lambda$) have been estimated and summarized for each sample in the Appendix.

RESULTS AND DISCUSSION

The Silicon-Boron System

Figure 1 shows the phase diagram for the silicon-boron system.[6] The maximum solubility for boron in silicon is indicated at about 3 a/o and occurs at about 1385 °C. In equilibrium, a silicon-boron sample below 1385 °C containing more than 3 a/o boron and less than about 75 a/o boron will consist of a mixture of 2 phases. One phase will be silicon saturated with boron (some amount <u>less</u> than 3 a/o boron) and the other phase will be either SiB_6 or SiB_3, depending on whether the sample is above 1270 °C (the decomposition temperature for SiB_3) or below. There is no question that such a sample will not contain any free boron in equilibrium.

The samples prepared in this study, of course, are not in equilibrium in the as-hot-pressed condition and extensive annealing studies are planned in order to bring about near equilibrium conditions. Never-the-less, the maximum solubility limit is not expected to be exceeded in solution and any silicon sample containing more than about 3 a/o boron will be expected to consist of more than one phase. Silicon has an atomic density of about 5×10^{22} atoms/cm^3. So 3 a/o of boron would contribute about 1.5×10^{21} cm^{-3} of holes, which is much greater than has been observed to date in any p-type specimen. Presumably, if measurements could be performed near the maximum solubility temperature of 1385 °C carrier concentrations on this order might be observed. At lower temperatures boron is much less soluble and much lower carrier concentrations are observed.

The actual boron concentration in solution resulting in a sample with more than 3 a/o boron available will depend on the kinetics of the boron

precipitation process, the temperature history of the sample and the solubility of boron as a function of temperature. The kinetics will depend on diffusion rates and the number of nucleation sites such as impurities, dislocations, grain boundaries and other point, line and plane defects. The kinetics of precipitation can therefore be expected depend on sample preparation conditions. The solubility, however, depends only on the local temperature and chemical composition and not at all on the preparation conditions. As a sample is cooled, the kinetics of precipitation will decrease quite rapidly. The final boron concentration at low temperatures will correspond roughly to the solubility of boron at the temperature at which the boron precipitation ceases to occur at an appreciable rate. Thus, similarly prepared samples with excess boron will be expected to have similar (but probably not identical) boron concentrations is solution.

Seebeck Coefficient in Silicon-Boron Samples

Figure 2 shows the Seebeck coefficient as a function of temperature for five silicon (T450, T467, T464, T479 and T468) samples containing 0 to 20 a/o boron. The sample with no added boron has a large, negative Seebeck coefficient which decreases in absolute magnitude with increasing temperature. The negative sign is consistent with the larger electron mobility compared to the hole mobility in silicon and the decrease in absolute magnitude with increasing temperature is consistent with the thermal excitation of carriers.

The sample with 0.001 atom fraction boron shows a large (about 500 μV/K at low temperatures) Seebeck coefficient which decreases with increasing temperature, while the final three samples with 0.01, 0.1 and 0.2 atom fraction boron have nearly the same, temperature independent Seebeck coefficient value of about 250 μV/K, at least on the scale of Figure 2. This is consistent with the interpretation that the samples with 0.01, 0.1 and 0.2 atom fraction boron are saturated with boron at the temperature at which boron ceases to precipitate, while essentially all of the boron in the 0.001 atom fraction boron sample is in solution. Figure 3 shows the same Seebeck coefficient data on an expanded scale. The Seebeck coefficient actually increases in the sequence 0.01, 0.1, 0.2 atom fraction boron. This is not consistent with the expectation that more boron supplied should, if anything, increase the amount of boron in solution and lower the Seebeck coefficient of the major Si(B) phase for that reason. A possible explanation for this trend is that the excess boron precipitates in a second phase with a large, positive Seebeck coefficient. Micrographs (see Ref. 5) do show increasing amounts of a boron-rich second phase in these samples. Either SiB_6 or SiB_3, the expected second phase compound(s), are high resistance, high Seebeck p-type semiconductors and therefore are consistent with this interpretation.

Electrical Resistivity in Silicon-Boron Samples

Figure 4 shows the electrical resistivity of five silicon (T450, T467, T464, T479 and T468) samples containing 0 to 20 a/o boron. As expected based upon the high Seebeck values, the samples containing 0.0 and 0.001 atom fraction boron have relatively large electrical resistivity values which approach a common value at very high temperatures. The high temperature behavior is typical of nearly intrinsic behavior. The sample with 0.2 atomic fraction boron shows the highest electrical resistivity, which again is inconsistent with the notion that more boron increases the boron concentration in solution, but is consistent with the formation of a high resistance second phase such as SiB_6.

The resistivity of the sample with 0.01 boron is higher than the sample with 0.1 boron, contrary to the trend in the Seebeck coefficients. The influences of boron concentration and high resistance second phase formation need not affect the resistivity and Seebeck coefficient in precisely the same way, so the observed results might not represent a contradiction. A number of other explanations might be offered such as microcracks, experimental error etc., but there seems to be insufficient information to answer this question definitively.

Electrical Power Factor for Silicon-Boron Samples

Figure 5 shows the electrical power factor (S^2/ρ) for five silicon (T450, T467, T464, T479 and T468) samples containing 0 to 20 a/o boron. The power factor of the 0.1 atomic fraction boron sample is significantly higher than for any other sample. Indeed, the average power factor of this sample from 800 K to 1200 K is about 33 $\mu W/cm\text{-}K^2$, which is nearly 60% better than typical of p-type SiGe materials. The lightly doped samples (0.0 and 0.001 boron), naturally have quite low power factor values.

Hall Effect in Silicon-Boron Samples

Figures 6, 7 and 8 show the Hall coefficient, $R_H=1/n_He$, where n_H is the Hall carrier concentration, for five silicon samples (T450, T467, T464, T479 and T468) containing 0 to 20 a/o boron and one sample of $Si_{0.8}Ge_{0.2}$ (T475) with no boron added. The large, negative values of the Hall coefficients for the undoped Si and undoped $Si_{0.8}Ge_{0.2}$ are consistent with the low doping levels expected in these samples. The negative values result from the larger value of the electron mobility compared to the hole mobility in these materials. The sharp decrease in the absolute value of the Hall coefficient above about 900 K is consistent with the thermal excitation of carriers in these samples, while the smaller, positive, nearly temperature independent values of the Hall coefficient for the 0.001 and 0.2 boron samples are consistent with the extrinsic behavior expected in these heavily doped samples.

Figure 7 shows the Hall coefficient above 800 K for several samples on an expanded scale. The undoped samples of Si and $Si_{0.8}Ge_{0.2}$ show typical intrinsic behavior and the lower (absolute magnitude) of the Hall coefficient of the $Si_{0.8}Ge_{0.2}$ is consistent with the smaller band gap of this composition compared pure silicon. A smaller band gap results in thermal excitation of more carriers and therefore a lower Hall coefficient. The sample doped with 0.1 boron exhibits a nearly temperature independent Hall coefficient (on this scale) up to the highest temperatures, while the sample with 0.001 boron shows a decreasing Hall coefficient which actually becomes negative at the highest temperature data point. This indicates that this sample also is essentially intrinsic at 1000 ^{o}C.

Figure 8 shows the Hall coefficient for the three highest boron content

silicon samples. The Hall coefficient decreases in the sequence 0.01, 0.10 and 0.20 atomic fraction boron, indicating that adding more boron does in fact increase the carrier concentration. The main problem with this interpretation is that the same argument about the influence of second phase materials discussed with respect to the Seebeck coefficient might be applied to describe the Hall coefficient results, which would present a contradiction. It should be noted that the Seebeck measurements were performed at Thermo Electron on the entire hot pressed compact, while the Hall measurements were performed at JPL on 1 mm slices taken from the end of the compacts. It is possible that either the samples changed as a result of having previously been measured at high temperatures or that the slices have different properties compared to the compacts.

The Hall data in Figure 8 shows rather large changes after heating. The Hall coefficients have increased substantially after exposure to high temperatures, although the changes were too small to observe on the scale of Figures 6 and 7. The increase in Hall coefficient indicates precipitation of boron from the samples during cooling from about 1300 K and emphasizes the effect of thermal history on the sample properties.

Figure 9 shows the Hall mobility ($\mu_H=\sigma R_H$) of five silicon samples (T450, T467, T464, T479 and T468) samples containing 0 to 20 a/o boron. Note that the undoped silicon sample (x=0, T450) is n-type, while the remaining 4 samples are p-type. The Hall mobility for the undoped silicon sample increases from 300 K to a maximum at about 500 K and then decreases with increasing temperature. This behavior may be related to a switch from domination by impurity scattering at low temperatures to lattice scattering at high temperatures. The mobility of the four boron-doped samples decreases with increasing temperature and also decreases slightly (less than 20%) with increasing boron content.

The more rapid drop in Hall mobility above about 900 K for the lightly doped (x=0.001) sample is attributed to the onset of intrinsic behavior as evidenced in the Seebeck coefficient (Figure 2) and Hall coefficient (Figure 7) for this sample. The mobilities for the three heavily doped samples (x=0.01, 0.1 and 0.2) are very similar at the highest temperatures. The lattice scattering contribution to the mobility is expected to be very weakly concentration dependent, but strongly temperature dependent, while impurity scattering is quite strongly concentration dependent. Thus, theory expects that the mobility will be less concentration dependent at high temperatures than at low temperatures, as is observed here.

<u>Specific Heat in Silicon-Boron Samples</u>

Figure 10 shows the specific heat (C_p, in units of Joules per cubic centimeter) for five silicon samples (T450, T467, T464, T479 and T468) containing 0 to 20 a/o boron. The specific heat values for the low boron content samples (x=0.0, 0.001, 0.01) are in good agreement with each other, while the two samples with higher boron content (0.1 and 0.2) show significantly higher specific heat values.

The specific heat (heat capacity per unit volume) is most closely related to the number of atoms per unit volume. Each atom contributes nearly equally, regardless of the atomic species. While the mass densities are similar, the molar volume of boron is about 2.6 times smaller than the molar volume of silicon. A mixture of 0.2 atomic fraction boron and 0.8 atomic fraction silicon will have a molar volume about 14% less than for pure silicon. To first order, the specific heat of the mixture would be about 14% higher than for pure silicon, which is close to the observed increase. A knowledge of the molar volumes of the actual second phase materials should provide a somewhat better estimate, but the main point is that the

experimental trend of an increase in the specific heat with increasing boron content is expected theoretically.

Thermal Diffusivity and Thermal Thermal Conductivity in Silicon-Boron Samples

Figure 11 shows the thermal diffusivity (α) for five silicon samples (T450, T467, T464, T479 and T468) containing 0 to 20 a/o boron. The thermal diffusivity decreases monotonically with increasing temperature and also decreases monotonically with increasing boron content. Heavily doped silicon germanium alloys, where α is about 0.02 cm^2/s, typically show an upturn in the thermal diffusivity at the highest temperatures due a contribution from thermally excited minority carriers. Presumably this effect is present here as well, but is not observed due to the much higher diffusivity values ($\alpha \approx 0.06$ to 0.10 cm^2/s at 1250 K) compared to the alloys.

Figure 12 shows the thermal conductivity ($\lambda = \alpha C_p$) for the same silicon-boron samples shown in Figure 11 and the same discussion generally applies. Literature values for the thermal conductivity of undoped silicon[7] agree with the data for the undoped sample, x=0.0, to within about 5%, which is quite good agreement.

Dimensionless Figure of Merit in Silicon-Boron Samples

Figure 13 shows the dimensionless figure of merit ($ZT = S^2T/\rho\lambda$) for five silicon samples (T450, T467, T464, T479 and T468) containing 0 to 20 a/o boron. The n-type undoped sample (x=0.0) and the lightly doped p-type sample (x=0.001) have very low figure of merit values, typical of intrinsic materials. The more heavily doped samples (x=0.01, 0.1 and 0.2) have fairly respectable figure of merit values with a peak of about $ZT_{peak}=0.2$ for the x=0.1 sample. Conventional, hot pressed p-type silicon germanium alloys have $ZT_{peak} \cong 0.5$, which is only 2.5 times higher.

While boron-doped silicon samples have better power factors than typical of silicon germanium alloys, the thermal conductivity values are also higher to the extent that the figure of merit is lower. Annealing may be expected to improve the mobility somewhat and therefore increase the figure of merit, however sufficient improvement to overtake the silicon germanium alloys cannot be expected. The excess boron, beyond a few atomic percent, does not appear to go into solution but seems to neither grossly improve nor degrade the properties of these samples.

Seebeck Coefficient in Boron-doped Silicon-Germanium Samples

Figure 14 shows the Seebeck coefficient (S) for four samples of silicon germanium doped with 0.01 atomic fraction boron (T464, T478, T477 and T476) containing 0 to 0.1 atomic fraction germanium ($Si_{0.99-y}Ge_yB_{0.01}$ with $0 \le y \le 0.1$) and one sample of $Si_{0.64}Ge_{0.16}B_{0.20}$ (T437). General trends in the Seebeck coefficient data seem to be overwhelmed by sample preparation variations. Different hot pressing temperatures (from 1150 °C to 1250 °C), for example, were used to compensate for the varying germanium contents. Annealing under fixed conditions should help minimize the variations due to sample preparation and allow the underlying trends to be observed.

Electrical Resistivity in Boron-doped Silicon-Germanium Samples

Figure 15 shows the electrical resistivity (ρ) for four samples of silicon germanium doped with 0.01 atomic fraction boron (T464, T478, T477 and T476) containing 0 to 0.1 atomic fraction germanium and one sample of $Si_{0.64}Ge_{0.16}B_{0.20}$ (T437). As with the Seebeck coefficient results, no general trends are readily apparent, although the shape of the resistivity versus temperature curves are similar for most of the samples.

Electrical Power Factor in Boron-doped Silicon-Germanium Samples

Figure 16 shows the electrical power factor (S^2/ρ) for four samples of silicon germanium doped with 0.01 atomic fraction boron (T464, T478, T477 and T476) containing 0 to 0.1 atomic fraction germanium and one sample of $Si_{0.64}Ge_{0.16}B_{0.20}$ (T437). The power factor for the y=0.0 (boron-doped silicon) and y=0.01 (boron-doped silicon with 1% germanium) show significantly higher power factor values compared to the higher germanium content samples with 5% and 10% germanium (y=0.05 and y=0.1). This is consistent with the previous observation that the boron-doped silicon samples (discussed above) often have higher power factors than typical of silicon germanium alloys.

Hall Effect in Boron-doped Silicon-Germanium Samples

Figure 17 shows the Hall coefficient ($R_H \equiv 1/n_H e$) for four samples of silicon germanium doped with 0.01 atomic fraction boron (T464, T478, T477 and T476) containing 0 to 0.1 atomic fraction germanium and one sample of $Si_{0.64}Ge_{0.16}B_{0.20}$ (T437). The reason for the wide variation and lack of trend in Seebeck coefficient and electrical resistivity results is most readily accounted for by the wide variation in carrier concentration values as indicated by the Hall coefficient. Presumably the differences in sample preparation and thermal history are responsible for the carrier concentration variations since the four samples with y=0.00, 0.01, 0.05 and 0.10 atomic fraction germanium all have the same boron content of 0.01 (1 atomic percent). Some hysteresis is observed in the Hall coefficients as a result of heating. The drop in the Hall coefficient at high temperatures for the y=0.01, 0.10 and most evident for the y=0.05 sample is attributed to the thermal excitation of minority carriers. Both the hysteresis and onset of intrinsic behavior were also observed in the boron-doped silicon samples discussed above.

Figure 18 shows the Hall mobility ($\mu_H = \sigma R_H$) as a function of temperature for four samples of silicon germanium doped with 0.01 atomic fraction boron

(T464, T478, T477 and T476) containing 0 to 0.1 atomic fraction germanium and one sample of $Si_{0.64}Ge_{0.16}B_{0.20}$ (T437). The temperature dependence of the Hall mobility is very similar for all five samples. Generally the mobility is lower for the higher germanium content samples, reflecting the effect of alloy scattering.

This effect is shown in Figure 19 where the mobility of these five samples are plotted as a function of germanium content at 800 K and 1200 K. Note that the y=0.2 point actually represents the $Si_{0.64}Ge_{0.16}B_{0.20}$ sample and is only shown for comparison. The solid and dashed lines approximately represent expected theoretical shape (an inverse parabola) for alloy scattering. The experimental results suggest most of the suppression in the mobility occurs with the addition of only 1% of germanium. Caution should be exercised, however, since these samples are known to exhibit significant variations in doping level and are quite inhomogeneous, which could be obscuring the true compositional dependence of the mobility.

Specific Heat in Boron-doped Silicon-Germanium Samples

Figure 20 shows the specific heat (C_p) for four samples of silicon germanium doped with 0.01 atomic fraction boron (T464, T478, T477 and T476) containing 0 to 0.1 atomic fraction germanium and one sample of $Si_{0.64}Ge_{0.16}B_{0.20}$ (T437). The agreement between the specific heat results for the five samples is quite good, with the exception of the results at the highest temperatures where the spread is as much as 10% and represents experimental error, mostly associated with the use of different calibrations for the infrared detector and heat flux for different runs. Some difficulty was experienced during this period with the detector which exhibited erratic and changing output and has since been replaced. The results included here have been judged reasonably reliable.

Thermal Diffusivity and Thermal Conductivity
in Boron-doped Silicon-Germanium Samples

Figure 21 shows the thermal diffusivity (α) for four samples of silicon germanium doped with 0.01 atomic fraction boron (T464, T478, T477 and T476) containing 0 to 0.1 atomic fraction germanium and one sample of $Si_{0.64}Ge_{0.16}B_{0.20}$ (T437). The diffusivity decreases with increasing temperature and with increasing germanium content, consistent with the increased mass fluctuation scattering of phonons in the alloys.

The thermal conductivity, shown in Figure 22, ($\lambda=\alpha C_p$) indicates the same general trend as shown for the diffusivity in Figure 21. The thermal conductivity is still surprisingly large (about 100 mW/cm-K) for the y=0.1 (10%) germanium sample. This value is almost twice as large as typical of hot pressed p-type $Si_{0.8}Ge_{0.2}$ and will serve to suppress the figure of merit.

The compositional dependence of the thermal conductivity is shown in Figure 23 at 800 K and 1200 K. Note that the y=0.2 point actually represents the $Si_{0.64}Ge_{0.16}B_{0.20}$ sample and is only shown for comparison. The solid and dashed lines approximately represent the expected theoretical shape (an inverse parabola) for alloy scattering. As with the electrical mobility, the thermal conductivity initially drops quite rapidly with composition. Most of the effect of alloying seems to have occurred with the addition of the first few percent of germanium, except that the $Si_{0.64}Ge_{0.16}B_{0.20}$ sample shows a significantly lower thermal conductivity than might be estimated by extrapolation from the 4 samples with less germanium. As was noted with

respect to the electrical mobility, sample homogeneity and variations in preparation may be distorting the true shape of the curve and some sort of annealing could be performed to produce more homogeneous samples. Indeed, since standard SiGe has a thermal conductivity of about 50 mW/cm-K at y=0.2, annealing may well have the effect of lowering all of the thermal conductivity values.

Dimensionless Figure of Merit in Boron-doped Silicon-Germanium Samples

Figure 21 shows dimensionless figure of merit ($ZT=S^2T/\rho\lambda$) for four samples of silicon germanium doped with 0.01 atomic fraction boron (T464, T478, T477 and T476) containing 0 to 0.1 atomic fraction germanium and one sample of $Si_{0.64}Ge_{0.16}B_{0.20}$ (T437). The highest figure of merit (ZT=0.35) occurs for the $Si_{0.64}Ge_{0.16}B_{0.20}$ sample, although even this value is still well below the values typical of hot pressed p-type $Si_{0.8}Ge_{0.2}$ (ZT=0.5). The figure of merit of the other four samples is uniformly low and disappointing. Even several of the boron-doped silicon samples (with no germanium) had higher figure of merit values.

Since 1% boron is ample to provide sufficient carriers (about 5×10^{20} cm^{-3}) and it is known that figure of merit values of at least ZT=0.5 can be routinely achieved, the relatively poor performance of these samples is attributed to some feature of the sample preparation procedure. Annealing can be expected to increase the carrier concentration values by driving more boron into solution, decrease the thermal conductivity by improving the sample homogeneity and increase the electrical mobility by cleaning up the grain boundaries.

SUMMARY

The figure of merit has been determined for samples of silicon and silicon germanium with various amounts of boron doping. To date, samples have been characterized in the "as-hot-pressed" state in order to provide a basis for evaluating the effect of annealing on the thermoelectric properties. Microstructural examinations indicate the samples are relatively inhomogeneous, both with respect to the silicon/germanium ratio and with respect to the distribution of boron. Large excess amounts of boron (beyond the maximum solubility of about 3 atomic percent) appear in the form of second phase material.

In many cases systematic trends expected in thermoelectric properties have not been observed. This is particularly true of properties which are sensitive to the doping level, such as the electrical resistivity, Seebeck coefficient and Hall Coefficient. The doping level resulting in solution has been found to be sensitive to the thermal history of the sample and since each sample has experienced somewhat different thermal processes, significant and difficult to predict variations in the doping level have resulted. In order to make reliable conclusions regarding the compositional and doping dependence of these properties, a systematic annealing program will be required. It is particularly important that all samples which are to be compared receive virtually identical annealing in order to minimize the effect of thermal history.

The thermal conductivity has been found to be more well behaved than typical of the electrical properties. This is attributed to the weaker doping dependence of the thermal conductivity compared to the electrical properties. The thermal conductivity decreases with either increasing germanium or increasing boron content. Germanium, which is completely soluble in silicon, is much more effective in lowering the thermal conductivity than boron, which has a quite limited solubility. The initial

suppression of the thermal conductivity with addition of small amounts of Ge seems to be more rapid than might be expected based on the results on the higher Ge content samples. Further, the high Ge content samples (particularly T476, $Si_{0.89}Ge_{0.10}B_{0.01}$) have higher thermal conductivity values than might be expected based on known values for standard p-type $Si_{0.8}Ge_{0.2}$.

These discrepancies in the thermal conductivity results are attributed to inhomogeneities, particularly in the silicon-germanium alloys. As with the electrical property results, annealing should help to minimize or remove these discrepancies. The high thermal conductivity values and poor power factor values can probably both be improved by proper thermal processing to improve the sample homogeneity. The figure of merit values are therefore expected to be considerably improved by annealing.

Currently the figure of merit values are relatively poor. The highest figure of merit found in this study was ZT_{peak}=0.35, which can be compared to ZT_{peak}=0.5 for standard p-type $Si_{0.8}Ge_{0.2}$. The figure of merit of the boron-doped silicon samples (without germanium) were actually surprisingly high with ZT_{peak}=0.2 for one sample. Annealing can be expected to improve these values somewhat by improving the Hall mobility to near single crystal values, but some germanium doping seems to be required to produce usefully low thermal conductivity values. Significant improvements can be expected, particularly in the silicon-germanium alloy samples.

RECOMMENDATIONS FOR FUTURE EFFORT

Future efforts should concentrate first on annealing of the existing samples. Since the diffusion rates are relatively slow, the highest temperatures possible and very long times are recommended. The silicon boron phase diagram (Figure 1) indicates the SiB_3 forms at temperature below ~1270 ^{o}C, and the silicon germanium phase diagram indicates the solidus for $Si_{0.8}Ge_{0.2}$ is about 1285 ^{o}C. To avoid crossing phase boundaries during cooling it is desirable to perform the annealing below these two temperatures.

To provide some room for error, an annealing temperature of 1240 ^{o}C is suggested and this temperature should be slowly approached with a heating rate of about 20 ^{o}C/day between 960 ^{o}C and 1240 ^{o}C. This will allow some time for possible gross inhomogeneities (such as the germanium-rich region) to diffuse. A 1000 hour anneal is suggested to approach complete homogenization. The anneal should be performed in an inert atmosphere (such as a sealed fused-silica ampoule) or vacuum (such as a vacuum furnace) and a quench to room temperature should be performed following the anneal. The thermoelectric properties should be redetermined and the microstructure reexamined.

A second area of effort should concentrate on boron-doped silicon-germanium alloys between silicon and $Si_{0.8}Ge_{0.2}$. Three boron doping levels are suggested: 0.5, 1 and 5 atomic percent. The 5% boron samples are expected to contain boron-silicide precipitates in small amounts, but should otherwise be saturated with boron. Germanium contents of 0, 1, 5, 10, and 20 atomic percent are suggested. A total of 15 samples will be required, but four of these already exist. Based on the current experience, the new samples need not be characterized following the hot pressing but should be immediately annealed as described above. The as-hot pressed materials are too inhomogeneous and variable from sample to sample to be useful in a

systematic and comparative study.

The proposed program can be summarized as follows:

- o Anneal and re-characterize the existing samples of silicon and silicon-germanium, undoped and doped with boron

- o Prepare samples with 0.5, 1 and 5 atomic percent boron and 0, 1, 5, 10 and 20 atomic percent germanium and characterize these samples following high temperature annealing. (4 of the required 15 samples have already been prepared).

- o Apply existing theoretical models to the thermoelectric properties of the annealed, homogeneous samples to provide a better understanding p-type silicon-germanium alloys.

This proposed program will allow determination of the compositional dependence of all of thermoelectric properties and allow for the first time a reliable estimate of the optimum doping level and germanium content for silicon-rich, p-type silicon germanium alloys. Significant gains in figure of merit are anticipated, but just as importantly these results will provide an experimental and theoretical basis for understanding silicon-rich, p-type silicon germanium alloys.

REFERENCES

1. J. W. Vandersande, A. Borshchevsky, J. Parker and C. Wood, Seventh International Conference on Thermoelectric Energy Conversion, Arlington, Texas, March 16-18, 1988, p. 76.
2. J. W. Vandersande, C. Wood and S. L. Draper, Mat. Res. Soc. Symp. Proc. Vol. 97, 347 (1987).
3. N. Gunther, "Cross-Doping Effects in p-Type SiGe Alloys," Proceedings of the 1981 Working Group on Thermoelectrics, Pasadena, California, December 15-16, 1981, p. 101.
4. G. McLane, "Thermoelectric Properties and Structure of Si-Ge alloys doped with Group III-IV Compounds," Proceedings of the Fifth Working Group Meeting on Thermoelectrics, Pasadena, California, February 1986.
5. M. Platek, R. G. Masters, and V. Raag, "Army Material Research Program - Final Report," JPL Contract Number 957956, Report Number TE4436-58-88, 1988.
6. R. W. Olesinski and G. J. Abbaschian; Bull. Alloy Phase Diagrams, 5(5), Oct. 1984.
7. W. Fulkerson, J. P. Moore, R. S. Graves, and D. L. McElroy, Proceedings of the Sixth Conference on Thermal Conductivity, Dayton, Ohio, October 19-21, 1966, p. 429-478.

APPENDIX

This appendix contains tabular summaries of the thermophysical properties of ten samples prepared in this project. The Seebeck coefficient (S) and electrical resistivity (ρ) measurements reported were performed at Thermo Electron while the density (d), Hall mobility (μ_H), thermal diffusivity (α) and heat capacity (C_p) measurements reported were performed at JPL. Interpolation schemes appropriate to each of the measurements have been used to estimate the properties at 50 K intervals. The electrical power factor (S^2/ρ), thermal conductivity (λ), figure of merit ($Z=S^2/\rho\lambda$) and dimensionless figure of merit ($ZT=S^2T/\rho\lambda$) have been calculated for each sample at 50 K intervals from the interpolated estimates of the measured properties. Numerically integrated average values over the temperature range 800 K to 1300 K are also included in each table.

Sample #:	T-450		Hot Pressing Parameters		
Si	100	atomic %	Temperature:	1250	C
Ge	0	atomic %	time:	2	hours
B	0	atomic %	Number of pressings:		1
density:	2.304	g/cm3	Anneal:	none	

T	S	ρ	S^2/ρ	μ	α	Cp	λ	Z	ZT
K	μV/K	mΩ-cm	mW/K^2	cm^2/Vs	cm^2/s	J/cm^3	mW/cm-K	$10^{-3}/K$	1
300									
350				56.0					
400	-613.6			60.4					
450	-677.1	60.023	7.64	64.8					
500	-718.5	64.699	7.98	69.3					
550	-739.9	67.554	8.10	73.7					
600	-743.5	68.752	8.04	73.4					
650	-731.3	68.455	7.81	71.0	.2240				
700	-705.5	66.827	7.45	67.2	.2075				
750	-668.1	64.029	6.97	63.1	.1916				
800	-621.2	60.224	6.41	58.9	.1801				
850	-567.0	55.575	5.78	53.8	.1659				
900	-507.5	50.244	5.13	47.4	.1520	2.100	319.2	.016	.014
950	-444.8	44.394	4.46	40.9	.1424	2.078	295.8	.015	.014
1000	-381.0	38.188	3.80	33.6	.1316	2.094	275.6	.014	.014
1050	-318.3	31.788	3.19	27.4	.1252	2.062	258.2	.012	.013
1100	-258.7	25.358	2.64	21.6	.1193	2.060	245.8	.011	.012
1150	-204.4	19.058	2.19	17.6	.1144	2.160	247.0	.009	.010
1200	-157.4	13.053	1.90	14.2	.1096	2.199	240.9	.008	.009
1250	-119.8	7.505	1.91		.1047	2.235	234.0	.008	.010
1300					.0998	2.278	227.4		

Integrated Average Values From 800K-1300K

Ave.	-358.0	34.539	3.74	35.0	.1314	2.141	260.4	.012	.012

Sample #:	T-467		Hot Pressing Parameters		
Si	99.9	atomic %	Temperature:	1250	C
Ge	0	atomic %	time:	2	hours
B	.1	atomic %	Number of pressings:		1
density:	2.315	g/cm3	Anneal:	none	

T	S	ρ	S^2/ρ	μ	α	Cp	λ	Z	ZT
K	μV/K	mΩ-cm	mW/K^2	cm^2/Vs	cm^2/s	J/cm^3	mW/cm-K	$10^{-3}/K$	1
300				38.2					
350	513.4	16.281	16.19	37.1					
400	506.1	16.647	15.39	35.6					
450	501.5	17.375	14.47	32.5					
500	498.5	18.381	13.52	30.3					
550	496.2	19.580	12.57	28.4					
600	493.5	20.885	11.66	25.7					
650	489.7	22.211	10.80	24.2	.2422	1.786	432.7	.025	.016
700	483.6	23.473	9.96	22.1	.2148	1.854	398.2	.025	.018
750	474.3	24.586	9.15	19.7	.1959	1.931	378.4	.024	.018
800	460.9	25.463	8.34	17.6	.1797	1.991	357.9	.023	.019
850	442.3	26.021	7.52	17.4	.1658	2.030	336.6	.022	.019
900	417.7	26.172	6.67	14.5	.1546	2.086	322.7	.021	.019
950	386.1	25.833	5.77	12.4	.1462	2.142	313.2	.018	.018
1000	346.5	24.916	4.82	9.6	.1378	2.222	306.2	.016	.016
1050	297.8	23.338	3.80	6.2	.1309	2.272	297.4	.013	.013
1100	239.3	21.012	2.73	3.4	.1245	2.307	287.2	.009	.010
1150	169.9	17.853	1.62		.1184	2.271	268.9	.006	.007
1200	88.6	13.776	.57		.1140	2.298	262.0	.002	.003
1250					.1074	2.421	259.9		
1300									

Integrated Average Values From 800K-1300K

	S	ρ	S^2/ρ	μ	α	Cp	λ	Z	ZT
Ave.	316.6	22.709	4.65	11.6	.1379	2.204	301.2	.015	.014

Sample #: T-464

Si 99 atomic %

Ge 0 atomic %

B 1 atomic %

density: 2.33 g/cm3

Hot Pressing Parameters

Temperature: 1250 C

time: 2 hours

Number of pressings: 1

Anneal: none

T K	S μV/K	ρ mΩ-cm	S^2/ρ mW/K^2	μ cm^2/Vs	α cm^2/s	Cp J/cm^3	λ mW/cm-K	Z $10^{-3}/K$	ZT 1
300				39.8					
350	208.5	1.258	34.56	36.6					
400	214.5	1.343	34.28	33.6					
450	220.6	1.440	33.78	30.9					
500	226.5	1.548	33.15	28.8					
550	232.3	1.665	32.42	26.9					
600	238.0	1.790	31.64	23.8					
650	243.4	1.922	30.83	22.8	.1769	1.753	310.0	.099	.065
700	248.5	2.057	30.03	21.3	.1638	1.851	303.1	.099	.069
750	253.3	2.195	29.23	19.8	.1545	1.942	300.1	.097	.073
800	257.7	2.335	28.43	18.3	.1465	2.001	293.2	.097	.078
850	261.6	2.474	27.65	16.6	.1358	2.047	278.1	.099	.085
900	264.9	2.611	26.88	15.4	.1299	2.097	272.3	.099	.089
950	267.7	2.744	26.12	14.2	.1233	2.170	267.5	.098	.093
1000	269.9	2.872	25.36	13.4	.1158	2.263	262.0	.097	.097
1050	271.3	2.992	24.60	12.7	.1082	2.308	249.6	.099	.103
1100	272.0	3.104	23.84	11.6	.1047	2.296	240.5	.099	.109
1150	271.9	3.206	23.06		.0993	2.254	223.9	.103	.118
1200	271.0	3.296	22.27		.0947	2.351	222.8	.100	.120
1250	269.1	3.372	21.47		.0921	2.374	218.6	.098	.123
1300	266.2	3.433	20.64						

Integrated Average Values From 800K-1300

	S	ρ	S^2/ρ	μ	α	Cp	λ	Z	ZT
Ave.	267.6	2.949	24.58	14.6	.1150	2.216	252.8	.099	.101

Sample #:	T-479	
Si	90	atomic %
Ge	0	atomic %
B	10	atomic %
density:	2.284	g/cm3

Hot Pressing Parameters		
Temperature:	1173	C
time:	2	hours
Number of pressings:	1	
Anneal:	none	

T K	S μV/K	ρ mΩ-cm	S^2/ρ mW/K^2	μ cm^2/Vs	α cm^2/s	Cp J/cm^3	λ mW/cm-K	Z 10^{-3}/K	ZT 1
300	221.6	.853	57.54	35.5					
350	222.8	.924	53.73	32.5					
400	225.6	1.003	50.75	30.1					
450	229.5	1.088	48.42	27.7					
500	234.5	1.179	46.62	25.4					
550	240.2	1.276	45.20	23.1					
600	246.4	1.378	44.07	20.9					
650	252.9	1.483	43.11	19.5	.1351	2.086	281.8	.153	.099
700	259.3	1.592	42.25	18.3	.1238	2.123	262.9	.161	.112
750	265.6	1.702	41.42	17.3	.1141	2.179	248.6	.167	.125
800	271.3	1.815	40.55	16.1	.1076	2.242	241.2	.168	.134
850	276.2	1.927	39.59	14.4	.1013	2.303	233.3	.170	.144
900	280.2	2.040	38.49	13.4	.0957	2.322	222.2	.173	.156
950	282.9	2.152	37.20	12.4	.0908	2.333	211.8	.176	.167
1000	284.2	2.262	35.70	11.9	.0860	2.349	202.0	.177	.177
1050	283.7	2.370	33.96	11.5	.0824	2.328	191.9	.177	.186
1100	281.2	2.474	31.96	11.0	.0779	2.346	182.7	.175	.192
1150	276.5	2.575	29.69	10.7	.0742	2.375	176.2	.168	.194
1200	269.2	2.670	27.15	10.5	.0712	2.357	167.8	.162	.194
1250	259.3	2.760	24.35		.0691	2.359	163.1	.149	.187
1300	246.3	2.844	21.34						

Integrated Average Values From 800K-1300

	S	ρ	S^2/ρ	μ	α	Cp	λ	Z	ZT
Ave.	273.7	2.353	32.73	12.4	.0856	2.331	199.2	.170	.173

Sample #:	T-468	
Si	80	atomic %
Ge	0	atomic %
B	20	atomic %
density:	2.355	g/cm3

Hot Pressing Parameters		
Temperature:	1250	C
time:	2	hours
Number of pressings:	1	
Anneal:	none	

T K	S μV/K	ρ mΩ-cm	S^2/ρ mW/K^2	μ cm^2/Vs	α cm^2/s	Cp J/cm^3	λ mW/cm-K	Z $10^{-3}/K$	ZT 1
300	314.9	1.295	76.54	34.4					
350	295.7	1.364	64.13	31.0					
400	281.3	1.450	54.58	28.9					
450	271.2	1.553	47.37	26.8					
500	264.8	1.670	42.00	24.8					
550	261.7	1.800	38.05	22.8					
600	261.3	1.941	35.18	20.8	.1238	2.258	279.6	.126	.075
650	263.1	2.090	33.11	18.7	.1102	2.301	253.7	.131	.085
700	266.6	2.247	31.63	17.4	.1072	2.361	253.1	.125	.087
750	271.3	2.410	30.55	16.2	.0996	2.402	239.1	.128	.096
800	276.7	2.576	29.73	15.0	.0940	2.470	232.2	.128	.102
850	282.3	2.744	29.06	14.2	.0876	2.522	221.0	.132	.112
900	287.6	2.911	28.42	13.4	.0831	2.590	215.3	.132	.119
950	292.1	3.077	27.72	12.5	.0803	2.629	211.0	.131	.125
1000	295.2	3.240	26.90	10.5	.0766	2.644	202.6	.133	.133
1050	296.5	3.396	25.88	10.1	.0728	2.699	196.4	.132	.138
1100	295.4	3.546	24.61	8.8	.0694	2.800	194.3	.127	.139
1150	291.4	3.687	23.04	9.0	.0662	2.754	182.3	.126	.145
1200	284.1	3.816	21.15	9.3	.0638	2.753	175.6	.120	.145
1250	272.9	3.933	18.94		.0615	2.739	168.5	.112	.140
1300	257.3	4.036	16.41						

Integrated Average Values From 800K-1300

	S	ρ	S^2/ρ	μ	α	Cp	λ	Z	ZT
Ave.	284.7	3.360	24.71	11.4	.0755	2.660	199.9	.127	.130

Sample #:	T-478	
Si	98	atomic %
Ge	1	atomic %
B	1	atomic %
density:	2.335	g/cm3

Hot Pressing Parameters		
Temperature:	1175	C
time:	2	hours
Number of pressings:	2	
Anneal:	none	

T K	S μV/K	ρ mΩ-cm	S^2/ρ mW/K^2	μ cm^2/Vs	α cm^2/s	Cp J/cm^3	λ mW/cm-K	Z $10^{-3}/K$	ZT 1
300	245.4	1.444	41.69	34.1					
350	247.7	1.516	40.48	31.7					
400	251.3	1.609	39.23	29.2					
450	255.8	1.722	38.01	26.8					
500	261.2	1.852	36.84	24.8					
550	267.1	1.997	35.73	23.0					
600	273.3	2.153	34.69	21.4					
650	279.6	2.320	33.69	19.7	.1110	1.837	203.9	.165	.107
700	285.7	2.493	32.73	18.4	.1048	1.879	197.0	.166	.116
750	291.4	2.672	31.77	17.2	.1008	1.921	193.6	.164	.123
800	296.4	2.852	30.80	15.9	.0971	1.978	192.1	.160	.128
850	300.6	3.033	29.79	14.7	.0924	2.033	187.8	.159	.135
900	303.6	3.210	28.72	13.7	.0877	2.055	180.3	.159	.143
950	305.3	3.383	27.56	12.7	.0829	2.068	171.6	.161	.153
1000	305.4	3.548	26.29	11.8	.0790	2.108	166.5	.158	.158
1050	303.7	3.704	24.91	10.8	.0761	2.130	162.0	.154	.161
1100	300.0	3.847	23.39	10.1	.0728	2.124	154.6	.151	.166
1150	293.9	3.975	21.74	9.1	.0699	2.107	147.2	.148	.170
1200	285.3	4.085	19.93	8.2	.0682	2.122	144.6	.138	.165
1250	274.0	4.176	17.97	7.2	.0666	2.116	140.9	.128	.159
1300	259.6	4.245	15.88	6.2	.0652	2.120	138.2	.115	.149

Integrated Average Values From 800K-1300

Ave.	293.4	3.642	24.27	11.0	.0780	2.087	162.3	.148	.154

Sample #: T-477
Si 94 atomic %
Ge 5 atomic %
B 1 atomic %
density: 2.445 g/cm3

Hot Pressing Parameters
Temperature: 1150 C
time: 2 hours
Number of pressings: 2
Anneal: none

T K	S μV/K	ρ mΩ-cm	S^2/ρ mW/K^2	μ cm^2/Vs	α cm^2/s	Cp J/cm^3	λ mW/cm-K	Z $10^{-3}/K$	ZT 1
300	221.0	3.090	15.81	30.1					
350	224.2	3.175	15.83	28.4					
400	229.4	3.320	15.85	26.5					
450	236.1	3.516	15.86	24.6					
500	244.1	3.756	15.86	22.9					
550	252.8	4.031	15.85	21.1					
600	262.0	4.334	15.84	19.6					
650	271.3	4.654	15.81	18.4	.0722	1.849	133.6	.118	.077
700	280.2	4.986	15.74	17.1	.0696	1.900	132.2	.119	.083
750	288.4	5.319	15.64	15.8	.0665	1.923	127.9	.122	.092
800	295.5	5.647	15.47	14.7	.0644	1.965	126.6	.122	.098
850	301.2	5.960	15.22	13.7	.0607	1.984	120.5	.126	.107
900	305.0	6.250	14.89	12.8	.0579	2.005	116.1	.128	.115
950	306.6	6.510	14.44	11.8	.0551	2.029	111.8	.129	.123
1000	305.6	6.730	13.88	10.8	.0530	2.076	110.1	.126	.126
1050	301.6	6.903	13.18	9.8	.0511	2.099	107.3	.123	.129
1100	294.2	7.020	12.33	8.8	.0503	2.152	108.2	.114	.125
1150	283.1	7.074	11.33	7.7	.0490	2.135	104.6	.108	.125
1200	267.9	7.055	10.17	6.6	.0480	2.136	102.5	.099	.119
1250	248.1	6.956	8.85	5.5	.0484	2.176	105.3	.084	.105
1300	223.5	6.768	7.38	4.4	.0513	2.261	115.9	.064	.083

Integrated Average Values From 800K-1300

	S	ρ	S^2/ρ	μ	α	Cp	λ	Z	ZT
Ave.	284.8	6.625	12.47	9.7	.0536	2.093	111.7	.111	.114

Sample #:	T-476		Hot Pressing Parameters		
Si	89	atomic %	Temperature:	1150	C
Ge	10	atomic %	time:	2	hours
B	1	atomic %	Number of pressings:	2	
density:	2.611	g/cm3	Anneal:	none	

T	S	ρ	S^2/ρ	μ	α	Cp	λ	Z	ZT
K	μV/K	mΩ-cm	mW/K^2	cm^2/Vs	cm^2/s	J/cm^3	mW/cm-K	10^{-3}/K	1
300	171.1	1.931	15.16	31.0					
350	175.3	2.007	15.31	28.9					
400	180.9	2.114	15.48	27.1					
450	187.6	2.246	15.67	25.3					
500	195.2	2.401	15.87	23.4					
550	203.4	2.575	16.07	21.5					
600	212.0	2.765	16.26	20.0					
650	220.8	2.967	16.44	18.7	.0580	1.859	107.8	.152	.099
700	229.5	3.177	16.58	17.6	.0572	1.923	110.0	.151	.106
750	237.9	3.392	16.69	16.5	.0547	1.966	107.6	.155	.116
800	245.7	3.608	16.74	15.4	.0522	2.042	106.6	.157	.126
850	252.8	3.823	16.71	14.4	.0502	2.065	103.6	.161	.137
900	258.7	4.031	16.61	13.4	.0477	2.080	99.3	.167	.151
950	263.4	4.231	16.40	12.4	.0455	2.073	94.4	.174	.165
1000	266.6	4.417	16.09	11.5	.0442	2.117	93.5	.172	.172
1050	268.0	4.587	15.66	10.6	.0431	2.175	93.7	.167	.175
1100	267.4	4.737	15.09	9.7	.0427	2.233	95.4	.158	.174
1150	264.5	4.864	14.39	8.8	.0422	2.284	96.5	.149	.171
1200	259.2	4.964	13.53	7.9	.0415	2.260	93.7	.144	.173
1250	251.1	5.033	12.53	7.0	.0410	2.175	89.1	.141	.176
1300	240.0	5.068	11.37	6.1					

Integrated Average Values From 800K-1300

	S	ρ	S^2/ρ	μ	α	Cp	λ	Z	ZT
Ave.	258.0	4.487	15.01	10.7	.0450	2.150	96.6	.159	.162

Sample #: T-475
Si 80 atomic %
Ge 20 atomic %
B 0 atomic %
density: 2.884 g/cm3

Hot Pressing Parameters
Temperature: 1150 C
time: 2 hours
Number of pressings: 2
Anneal: none

T	S	ρ	S^2/ρ	μ	α	Cp	λ	Z	ZT
K	μV/K	mΩ-cm	mW/K^2	cm^2/Vs	cm^2/s	J/cm^3	mW/cm-K	$10^{-3}/K$	1
300	-683.2	697.2	0.67	17.8					
350	-733.6	587.6	.92	19.0					
400	-761.3	491.5	1.18	20.4					
450	-768.7	407.9	1.45	21.7					
500	-758.0	335.9	1.71	24.3					
550	-731.8	274.4	1.95	27.4					
600	-692.2	222.7	2.15	29.7					
650	-641.7	179.7	2.29	34.2					
700	-582.7	144.5	2.35	35.7					
750	-517.5	116.2	2.30	36.8					
800	-448.4	93.8	2.14	37.5					
850	-377.9	76.4	1.87	34.7					
900	-308.2	63.0	1.51	30.0					
950	-241.8	52.8	1.11	25.3					
1000	-181.0	44.7	.73	20.2					
1050	-128.1	37.8	.43	15.8					
1100	-85.5	31.2	.23	12.6					
1150	-55.6	24.0	.13	9.8					
1200	-40.7	15.2	.11	7.8					
1250				5.8					
1300				3.9					

Integrated Average Values From 800K-1300

	S	ρ	S^2/ρ	μ
Ave.	-207.5	48.8	.92	18.5

Sample #: T-437

Si	64	atomic %
Ge	16	atomic %
B	20	atomic %
density:	2.829	g/cm3

Hot Pressing Parameters

Temperature:	1175	C
time:	4	hours
Number of pressings:	2	
Anneal:	none	

T	S	ρ	S^2/ρ	μ	α	Cp	λ	Z	ZT
K	μV/K	mΩ-cm	mW/K^2	cm^2/Vs	cm^2/s	J/cm^3	mW/cm-K	10^{-3}/K	1
300	121.9	1.082	13.74	29.3					
350	131.4	1.160	14.89	26.4					
400	140.7	1.245	15.89	25.3					
450	149.7	1.337	16.76	24.2					
500	158.4	1.435	17.49	22.7					
550	166.8	1.537	18.10	21.2					
600	174.9	1.645	18.59	18.5					
650	182.5	1.756	18.98	17.9	.0349				
700	189.8	1.870	19.27	16.7	.0342				
750	196.6	1.986	19.46	15.4	.0340				
800	202.9	2.105	19.57	14.2	.0327	2.0712	67.8	.289	.231
850	208.7	2.224	19.59	13.3	.0313	2.0825	65.3	.300	.255
900	214.0	2.344	19.54	12.4	.0300	2.1142	63.3	.309	.278
950	218.7	2.464	19.41	11.5	.0291	2.1622	62.9	.309	.293
1000	222.8	2.583	19.22	10.9	.0285	2.2433	63.9	.301	.301
1050	226.2	2.700	18.95	10.0	.0275	2.2022	60.6	.313	.328
1100	229.0	2.815	18.63	9.6	.0264	2.2175	58.5	.318	.350
1150	231.0	2.927	18.24	9.0	.0261	2.3818	62.3	.293	.337
1200	232.3	3.035	17.78	8.4	.0258	2.4522	63.2	.281	.338
1250				7.8	.0260	2.4833	64.6		
1300				7.2					

Integrated Average Values From 800K-1300

	S	ρ	S^2/ρ	μ	α	Cp	λ	Z	ZT
Ave.	220.6	2.577	18.99	10.4	.0283	2.241	63.2	.301	.301

FIGURES

Figure 1: The boron-silicon phase diagram.[6]

Figure 2: The Seebeck Coefficient as a function of temperature for four samples of boron-doped silicon and one sample of undoped silicon.

Figure 3: The Seebeck Coefficient as a function of temperature for four samples of boron-doped silicon.

Figure 4: The electrical resistivity as a function of temperature for four samples of boron-doped silicon and one sample of undoped silicon. Note the much higher resistance of the undoped and 0.001 atom fraction boron-doped samples compared to the three more heavily doped samples.

Figure 5: The electrical power factor (S^2/ρ) as a function of temperature for four samples of boron-doped silicon and one sample of undoped silicon. The undoped silicon sample is n-type, while the four boron-doped samples are p-type.

Figure 6: The Hall coefficient ($1/n_H e$) as a function of inverse temperature for two samples of boron-doped silicon, one sample of undoped silicon and one sample of undoped $Si_{0.8}Ge_{0.2}$. The left and right arrows indicate data taken while heating and cooling, respectively.

Figure 7: The Hall coefficient ($1/n_H e$) as a function of inverse temperature above from 800 K to 1300 K for two samples of boron-doped silicon, one sample of undoped silicon and one sample of undoped $Si_{0.8}Ge_{0.2}$. Note that the 0.001 atomic fraction boron sample changes from p-type to n-type at the highest temperatures

Figure 8: The Hall coefficient ($1/n_H e$) as a function of inverse temperature for three samples of boron-doped silicon. The left and right arrows indicate data collected while the sample temperature was increasing and decreasing, respectively. Note that the Hall coefficient is significantly higher (carrier concentration lower) during cooling compared to the warming data.

Figure 9: The Hall mobility as a function of temperature for four samples of boron-doped silicon and one sample of undoped silicon. The undoped silicon sample is n-type, while the four boron-doped samples are p-type.

Figure 10: The heat capacity of four samples of boron-doped silicon and one sample of undoped silicon. The relatively high heat capacity of the 0.1 and 0.2 atom fraction boron samples is attributed to the increased atom-density of these samples.

Figure 11: The thermal diffusivity as a function of temperature for four samples of boron-doped silicon and one sample of undoped silicon. The thermal diffusivity decreases with increasing boron content.

Figure 12: The thermal conductivity as a function of temperature for four samples of boron-doped silicon and one sample of undoped silicon. The thermal conductivity decreases with increasing boron content.

Figure 13: The dimensionless figure of merit ($S^2T/\rho\lambda$) as a function of temperature for four samples of boron-doped silicon and one sample of undoped silicon. The undoped silicon sample is n-type, while the four boron-doped samples are p-type.

Figure 14: The Seebeck Coefficient as a function of temperature for five samples of boron-doped silicon-germanium.

Figure 15: The electrical resistivity as a function of temperature for five samples of boron-doped silicon-germanium.

Figure 16: The electrical power factor (S^2/ρ) as a function of temperature for five samples of boron-doped silicon-germanium.

Figure 17: The Hall coefficient (1/ne) as a function of inverse temperature for five samples of boron-doped silicon-germanium. The left and right arrows indicate data collected while the sample temperature was increasing and decreasing, respectively. Note that the Hall coefficient higher (carrier concentration lower) during cooling compared to the warming data.

Figure 18: The Hall mobility as a function of temperature for five samples of boron-doped silicon-germanium. Note that the mobility generally decreases as the germanium content increases.

Figure 19: The Hall mobility as a function of germanium content for five samples of boron-doped silicon-germanium at 800 K and 1200 K. The mobility generally decreases as the germanium content increases, but the agreement with simple theory, given by the lines, is qualitatively poor.

Figure 20: The heat capacity of five samples of boron-doped silicon-germanium. The somewhat larger variation in heat capacities observed at the highest temperatures is attributed to experimental uncertainties, but represents only modest absolute errors for this type of measurement.

Figure 21: The thermal diffusivity as a function of temperature for five samples of boron-doped silicon-germanium. The thermal diffusivity decreases with increasing germanium content.

Figure 22: The thermal conductivity as a function of temperature for five samples of boron-doped silicon-germanium. The thermal conductivity decreases with increasing germanium content.

Figure 23: The thermal conductivity as a function of germanium content for five samples of boron-doped silicon-germanium at 800 K and 1200 K. The thermal conductivity generally decreases as the germanium content increases, but the agreement with simple theory, given by the lines, is qualitatively poor.

Figure 24: The dimensionless figure of merit ($S^2T/\rho\lambda$) as a function of temperature for five samples of boron-doped silicon-germanium.

Figure 1: The boron-silicon phase diagram.[6]

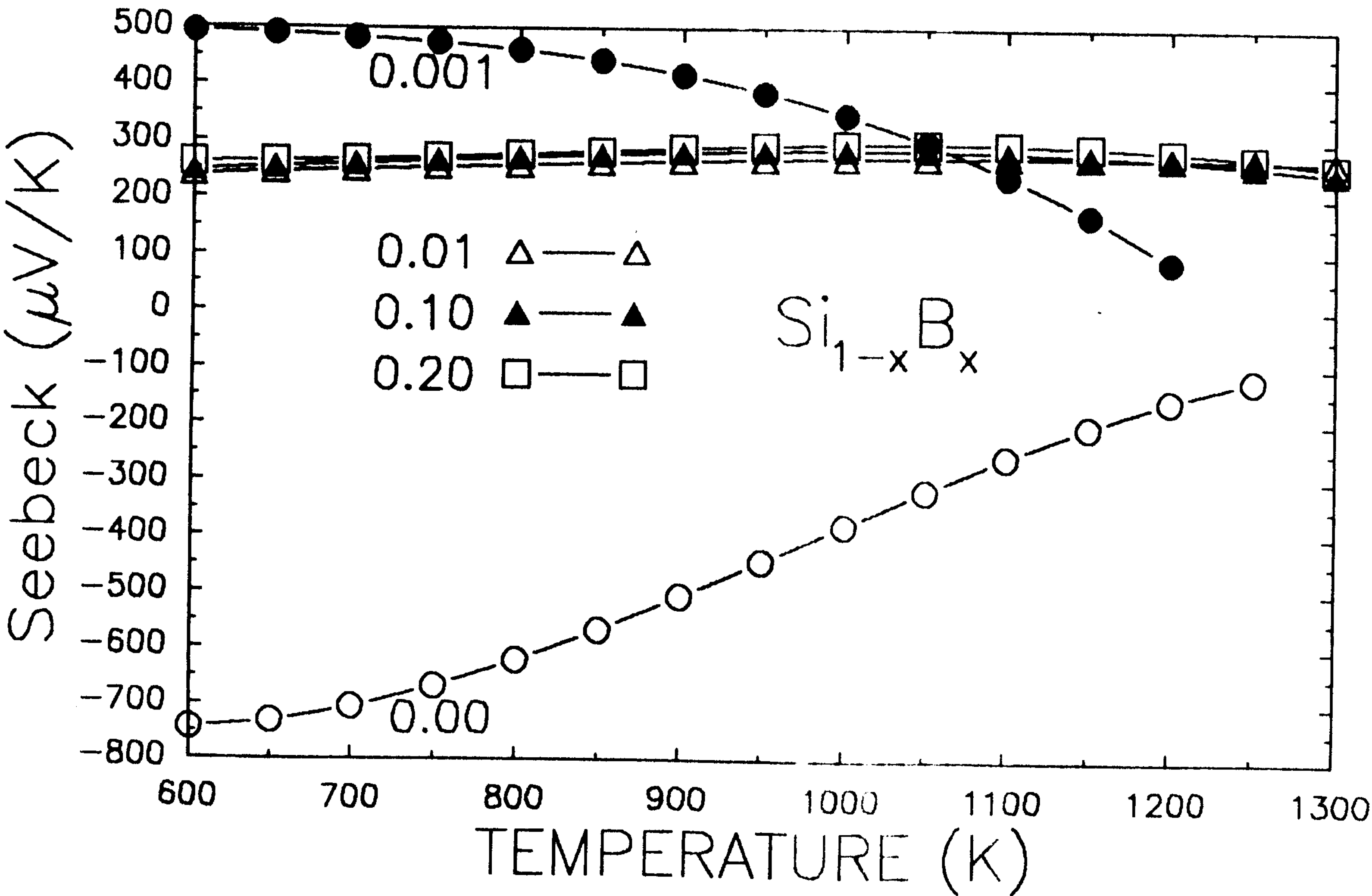

Figure 2: The Seebeck Coefficient as a function of temperature for four samples of boron-doped silicon and one sample of undoped silicon.

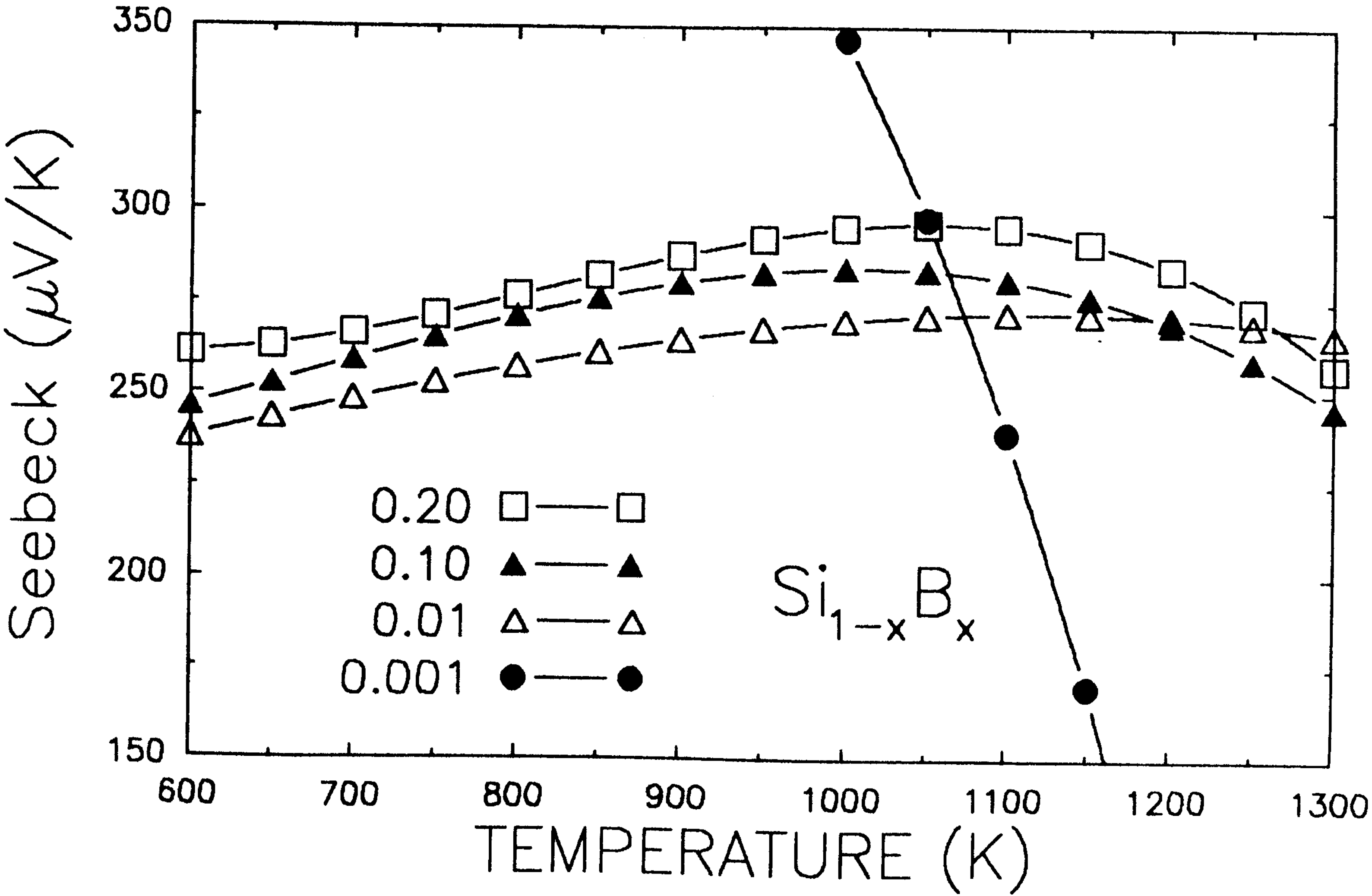

Figure 3: The Seebeck Coefficient as a function of temperature for four samples of boron-doped silicon.

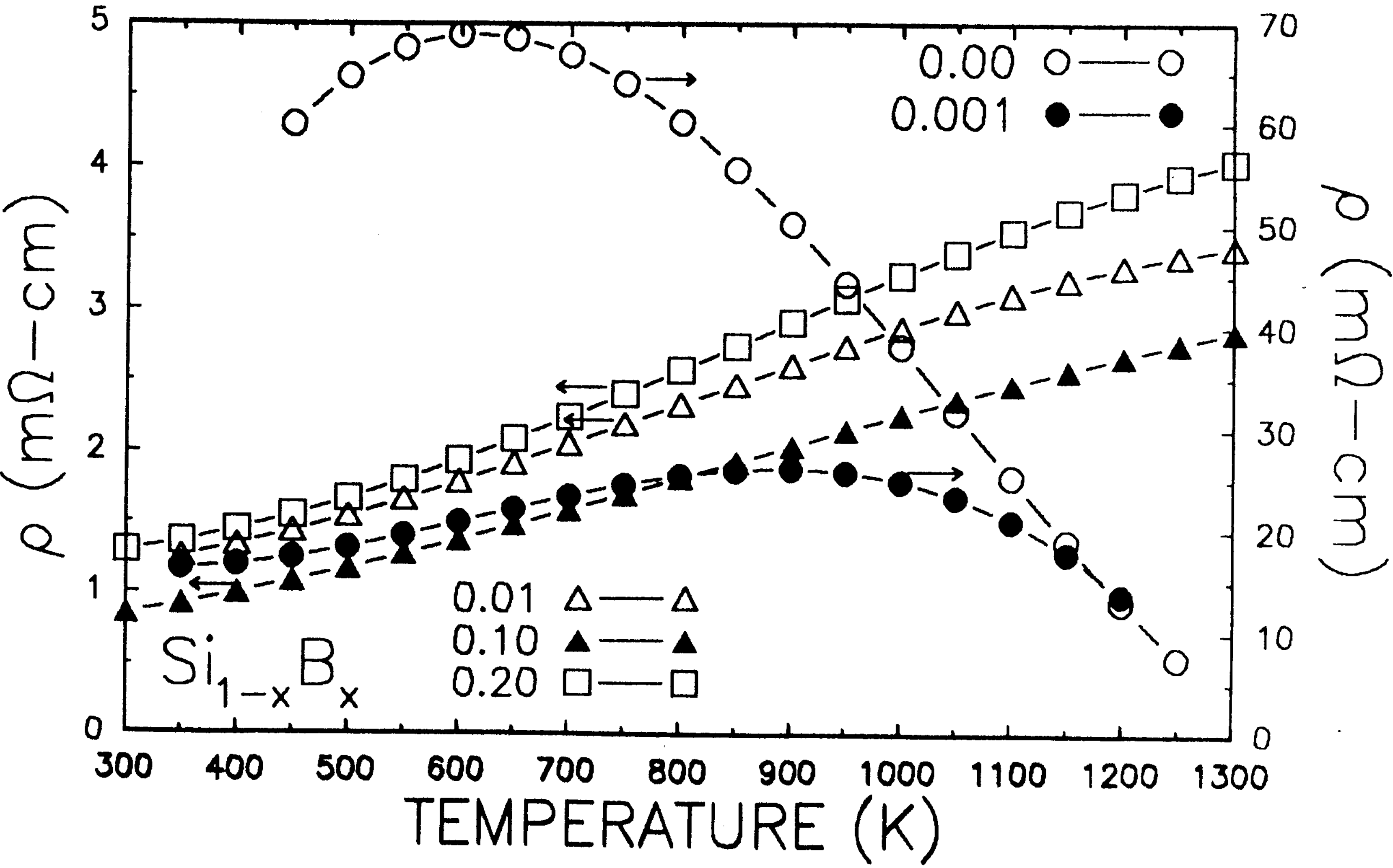

Figure 4: The electrical resistivity as a function of temperature for four samples of boron-doped silicon and one sample of undoped silicon. Note the much higher resistance of the undoped and 0.001 atom fraction boron-doped samples compared to the three more heavily doped samples.

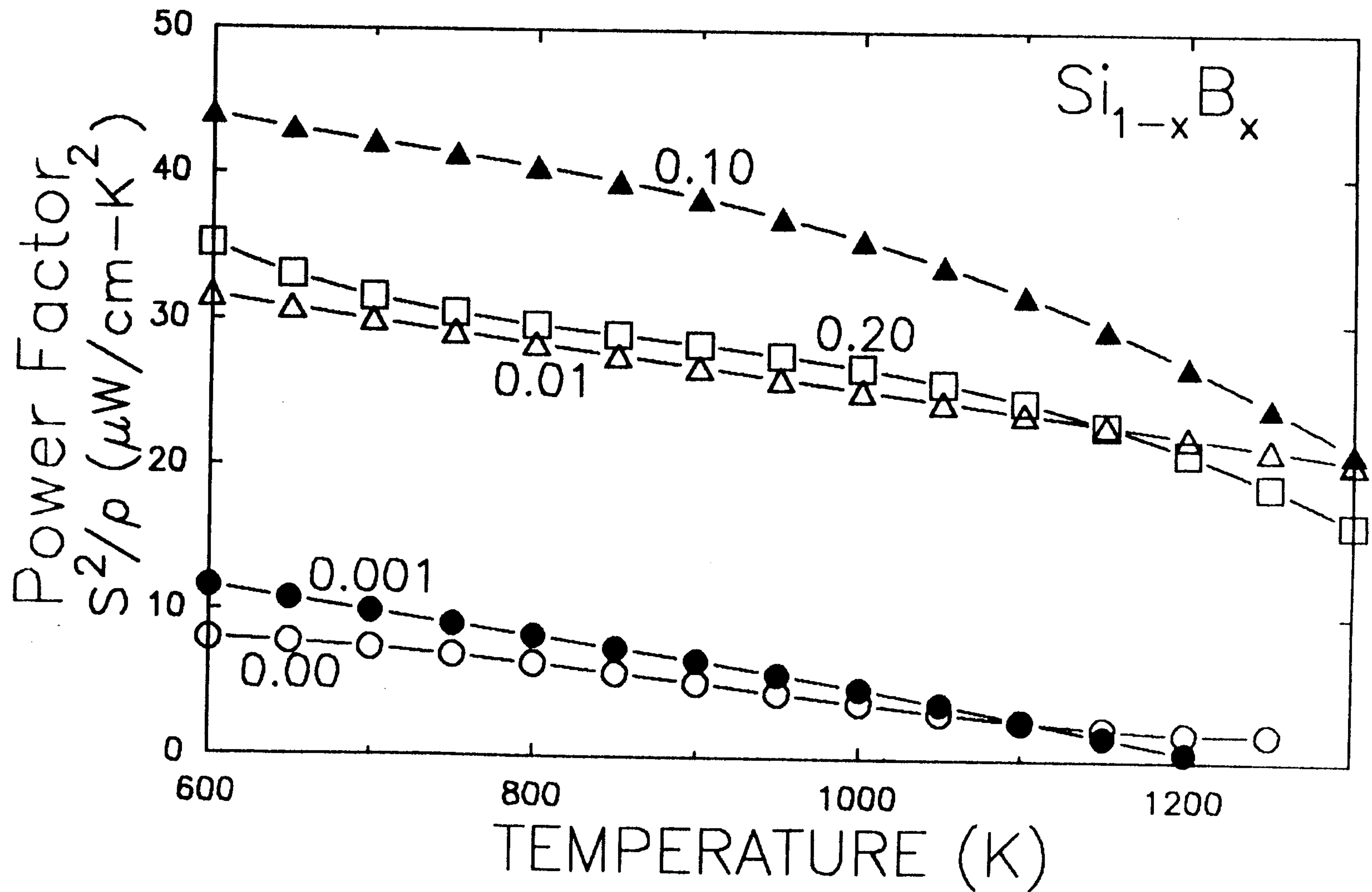

Figure 5: The electrical power factor (S^2/ρ) as a function of temperature for four samples of boron-doped silicon and one sample of undoped silicon. The undoped silicon sample is n-type, while the four boron-doped samples are p-type.

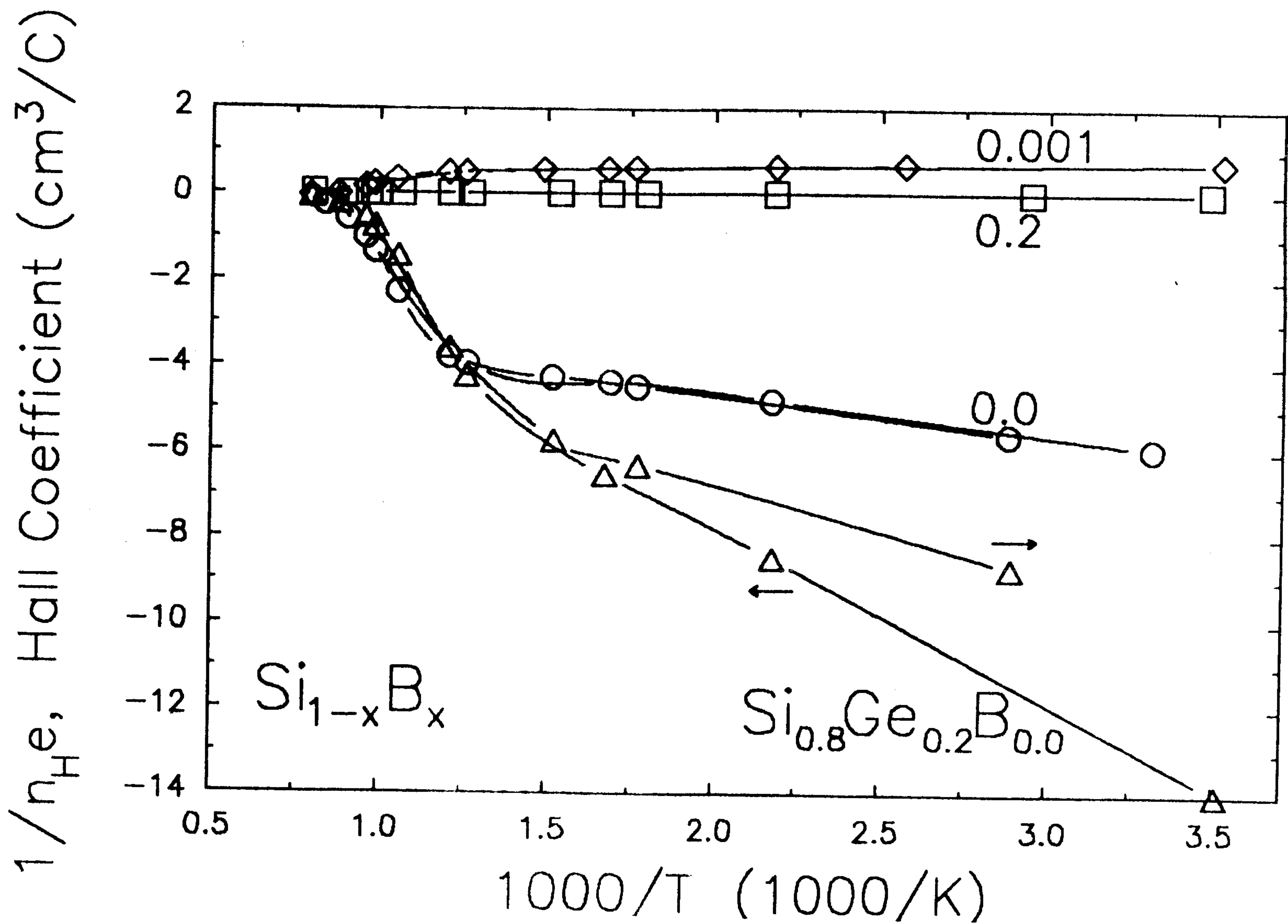

Figure 6: The Hall coefficient ($1/n_He$) as a function of inverse temperature for two samples of boron-doped silicon, one sample of undoped silicon and one sample of undoped $Si_{0.8}Ge_{0.2}$. The left and right arrows indicate data taken while heating and cooling, respectively.

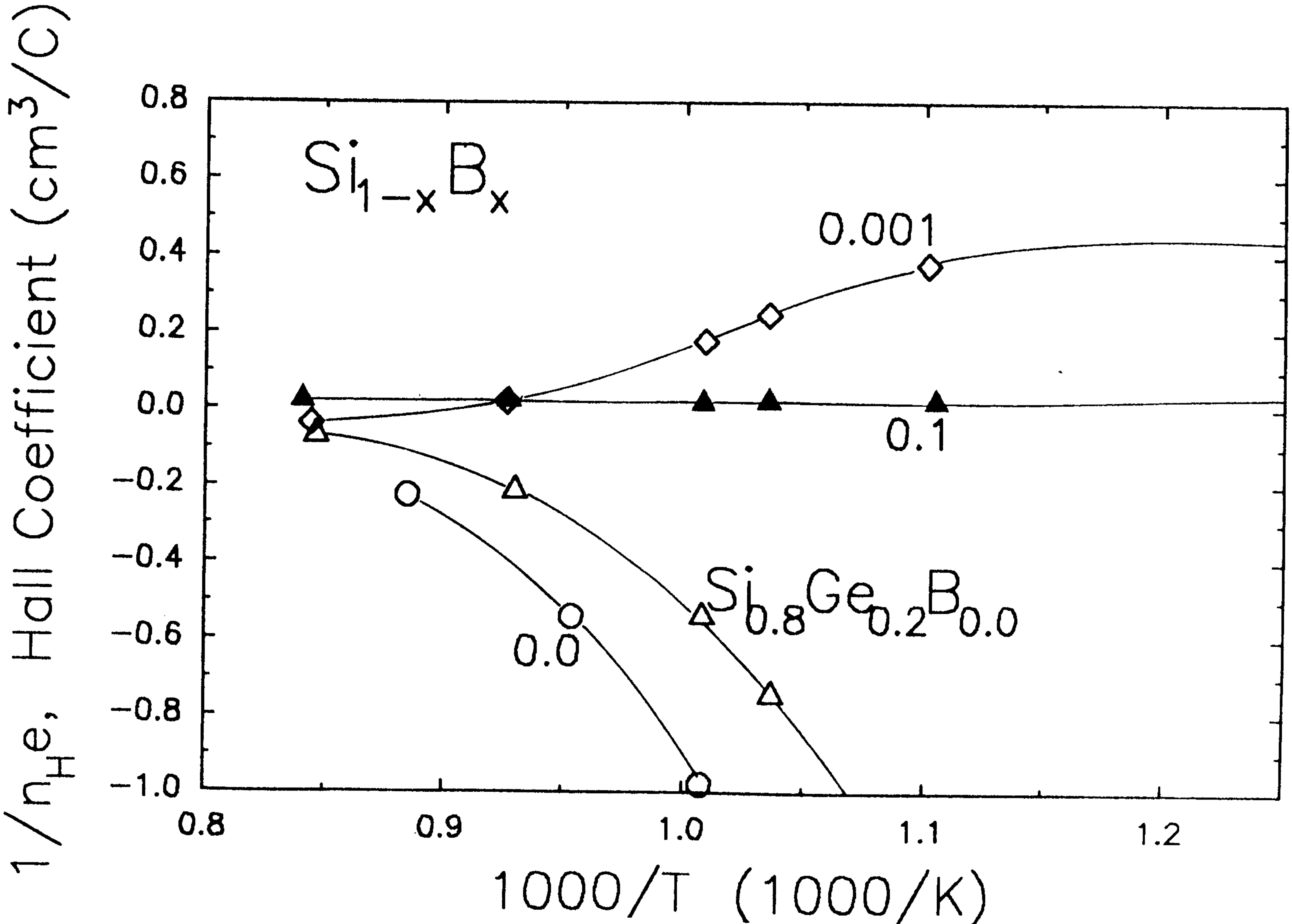

Figure 7: The Hall coefficient ($1/n_He$) as a function of inverse temperature above from 800 K to 1300 K for two samples of boron-doped silicon, one sample of undoped silicon and one sample of undoped $Si_{0.8}Ge_{0.2}$. Note that the 0.001 atomic fraction boron sample changes from p-type to n-type at the highest temperatures

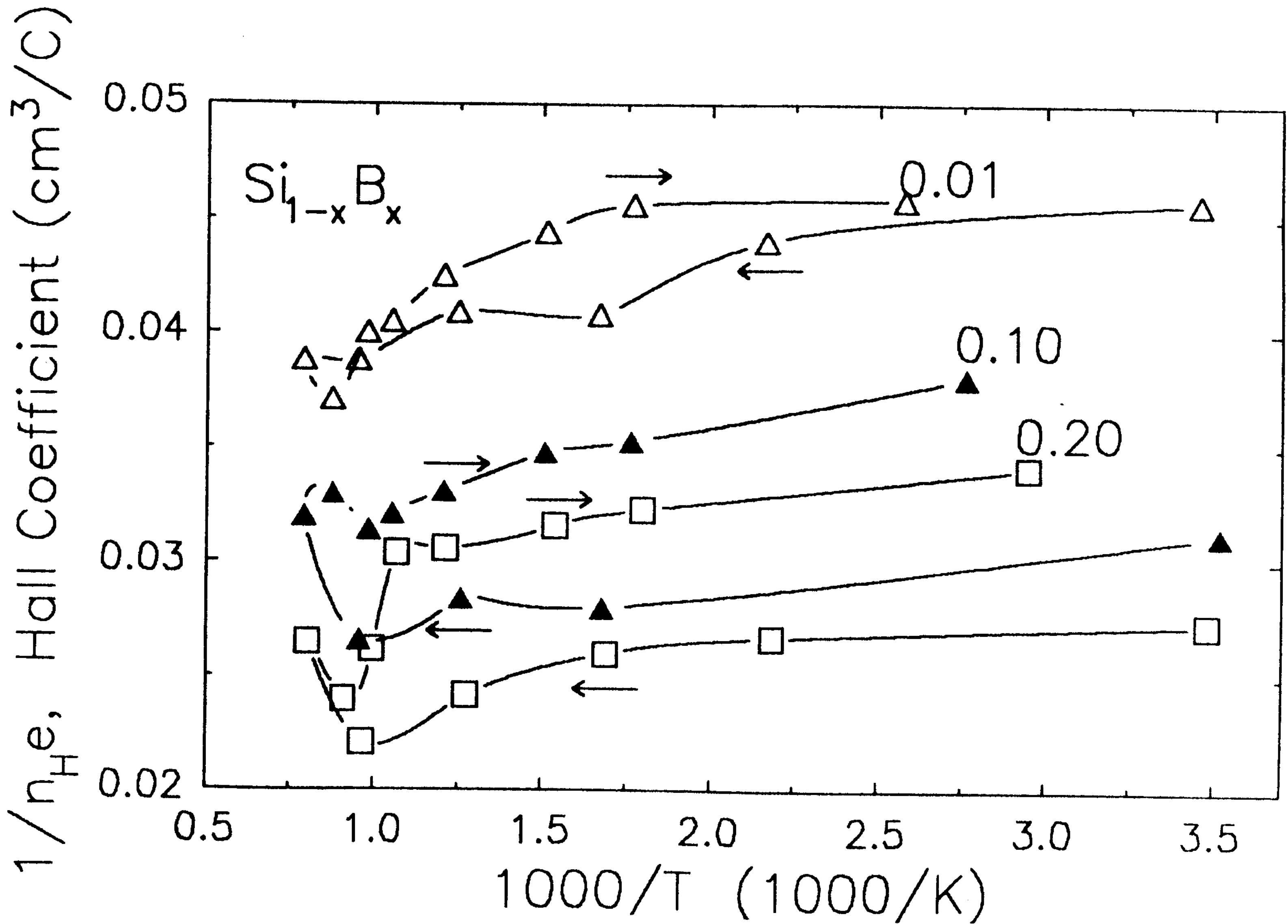

Figure 8: The Hall coefficient ($1/n_He$) as a function of inverse temperature for three samples of boron-doped silicon. The left and right arrows indicate data collected while the sample temperature was increasing and decreasing, respectively. Note that the Hall coefficient is significantly higher (carrier concentration lower) during cooling compared to the warming data.

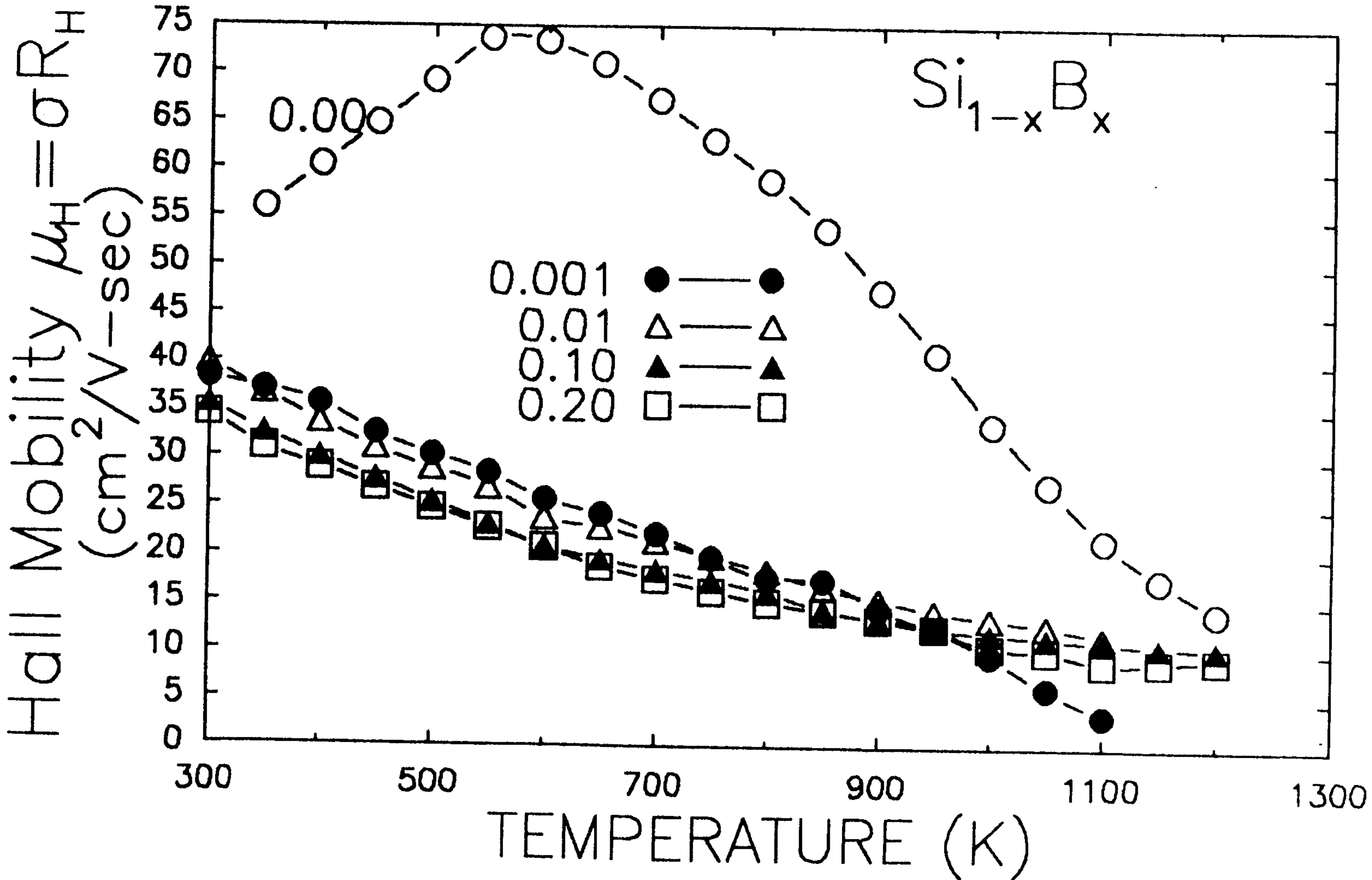

Figure 9: The Hall mobility as a function of temperature for four samples of boron-doped silicon and one sample of undoped silicon. The undoped silicon sample is n-type, while the four boron-doped samples are p-type.

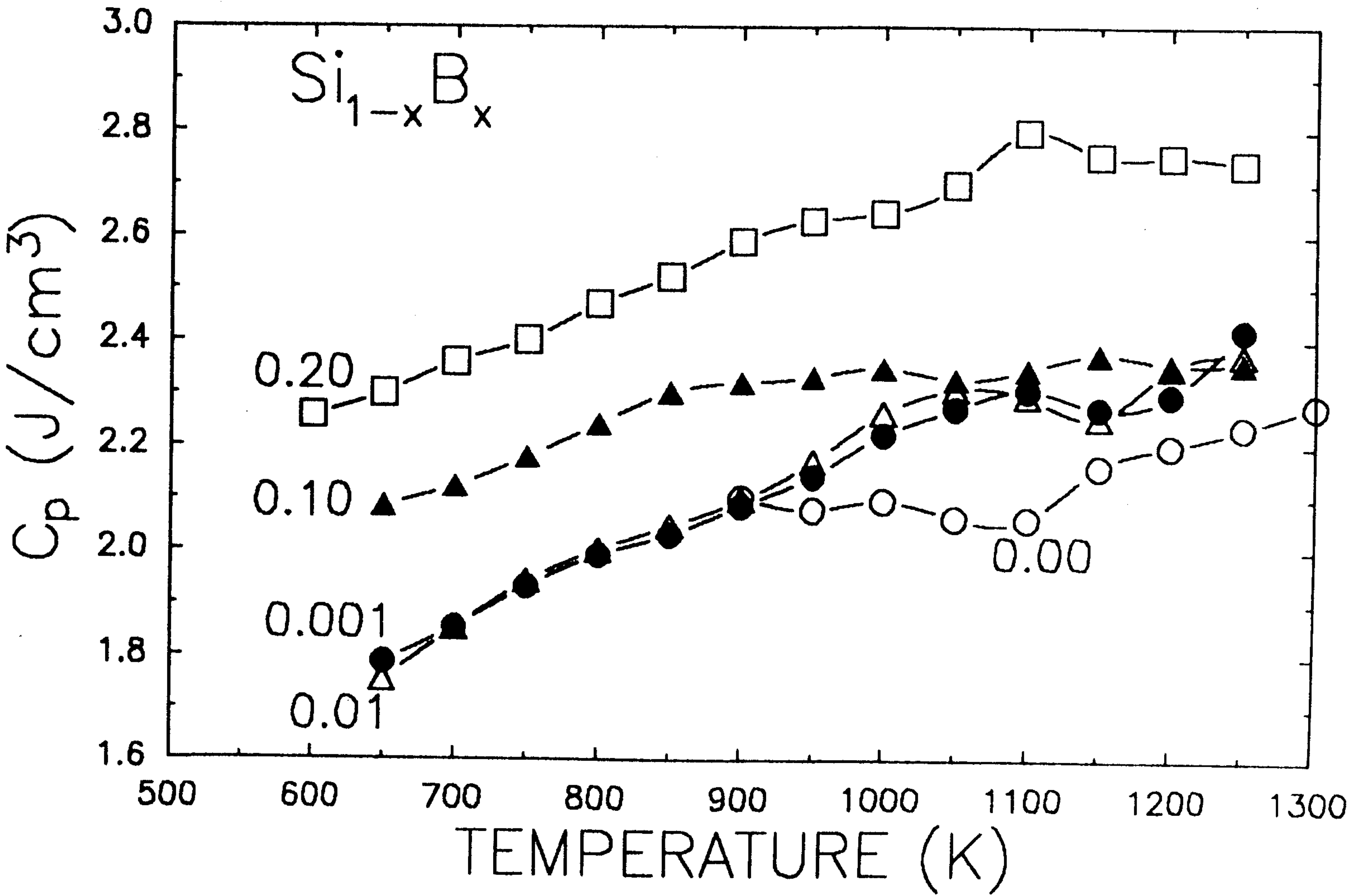

Figure 10: The heat capacity of four samples of boron-doped silicon and one sample of undoped silicon. The relatively high heat capacity of the 0.1 and 0.2 atom fraction boron samples is attributed to the increased atom-density of these samples.

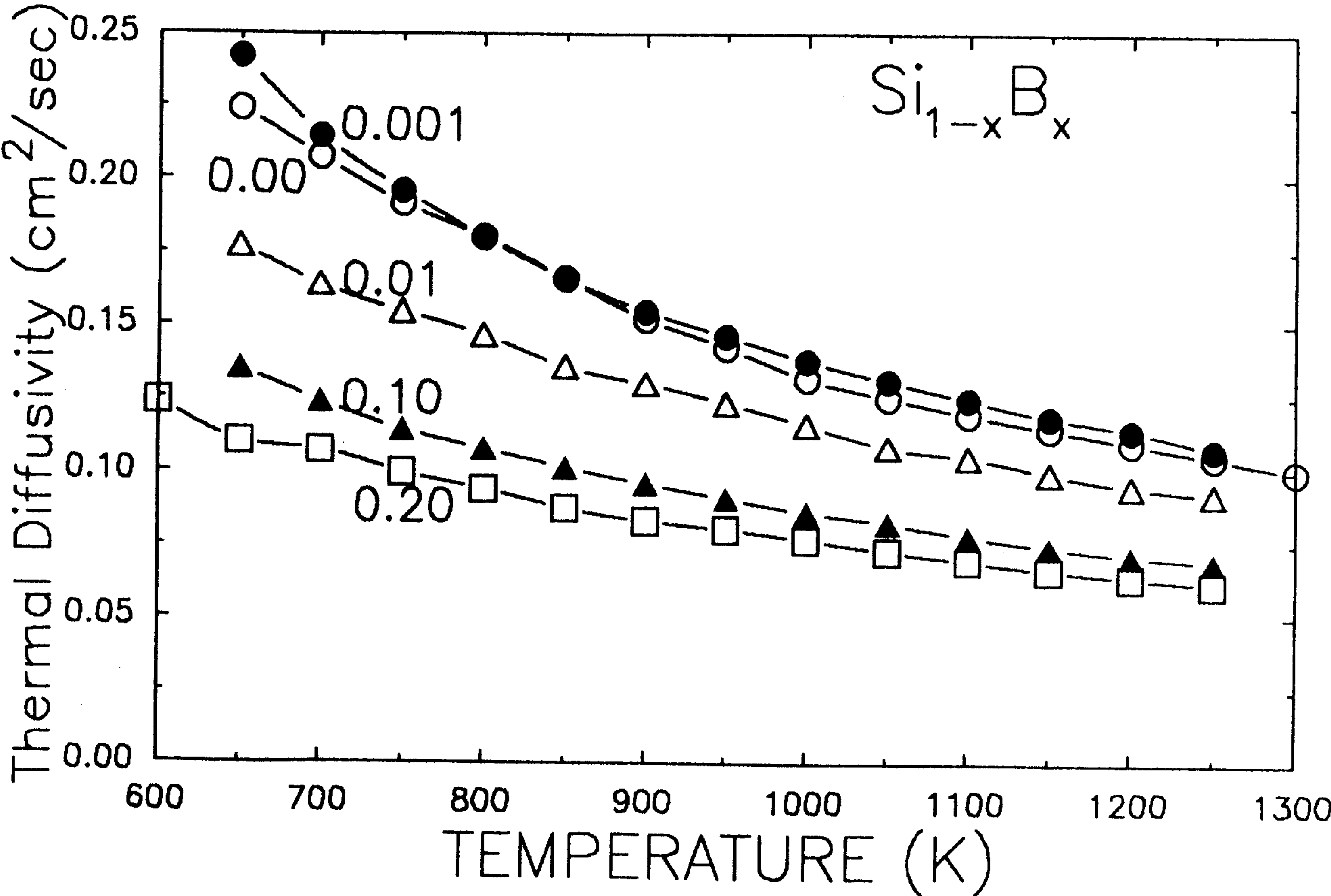

Figure 11: The thermal diffusivity as a function of temperature for four samples of boron-doped silicon and one sample of undoped silicon. The thermal diffusivity decreases with increasing boron content.

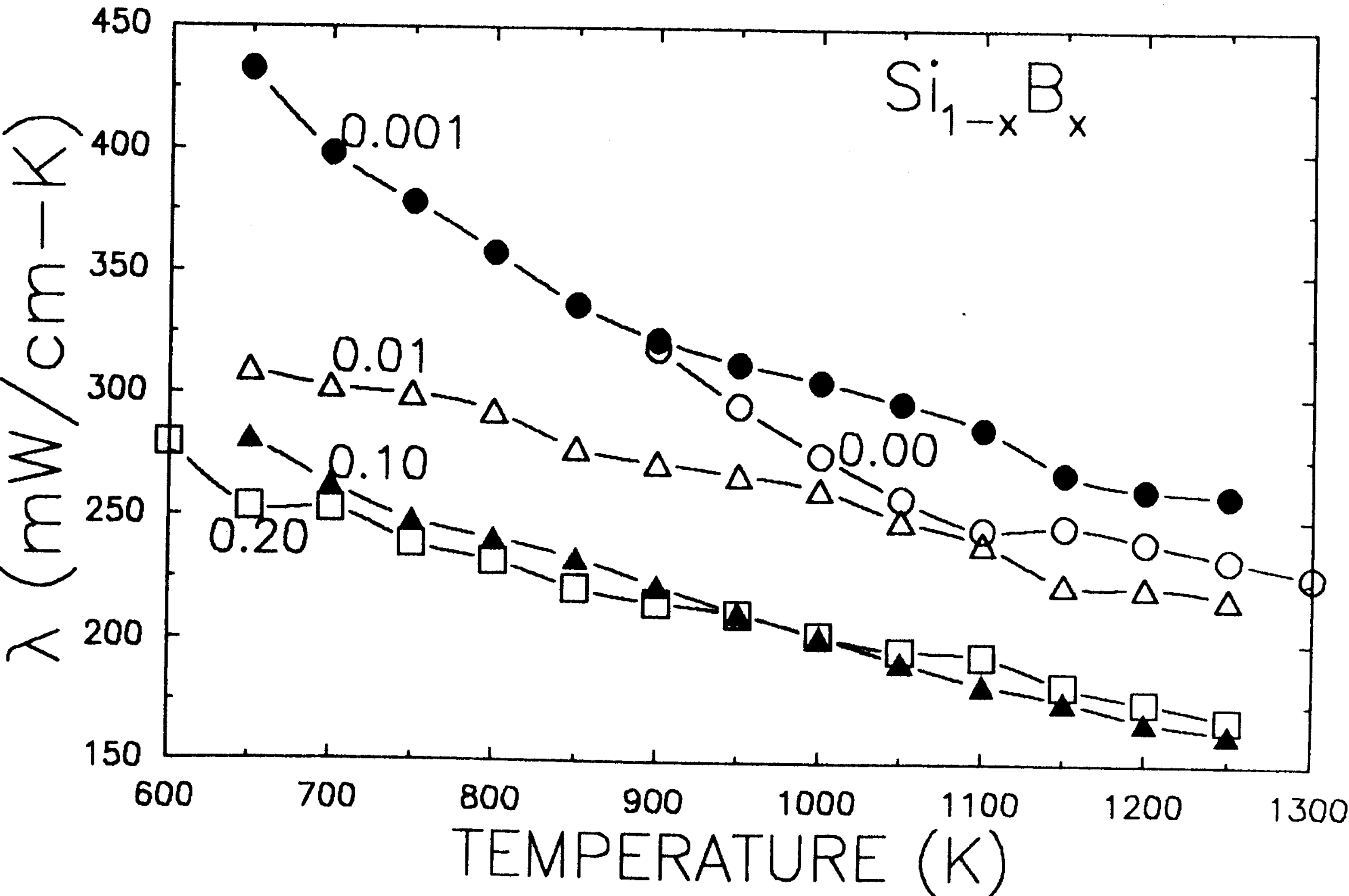

Figure 12: The thermal conductivity as a function of temperature for four samples of boron-doped silicon and one sample of undoped silicon. The thermal conductivity decreases with increasing boron content.

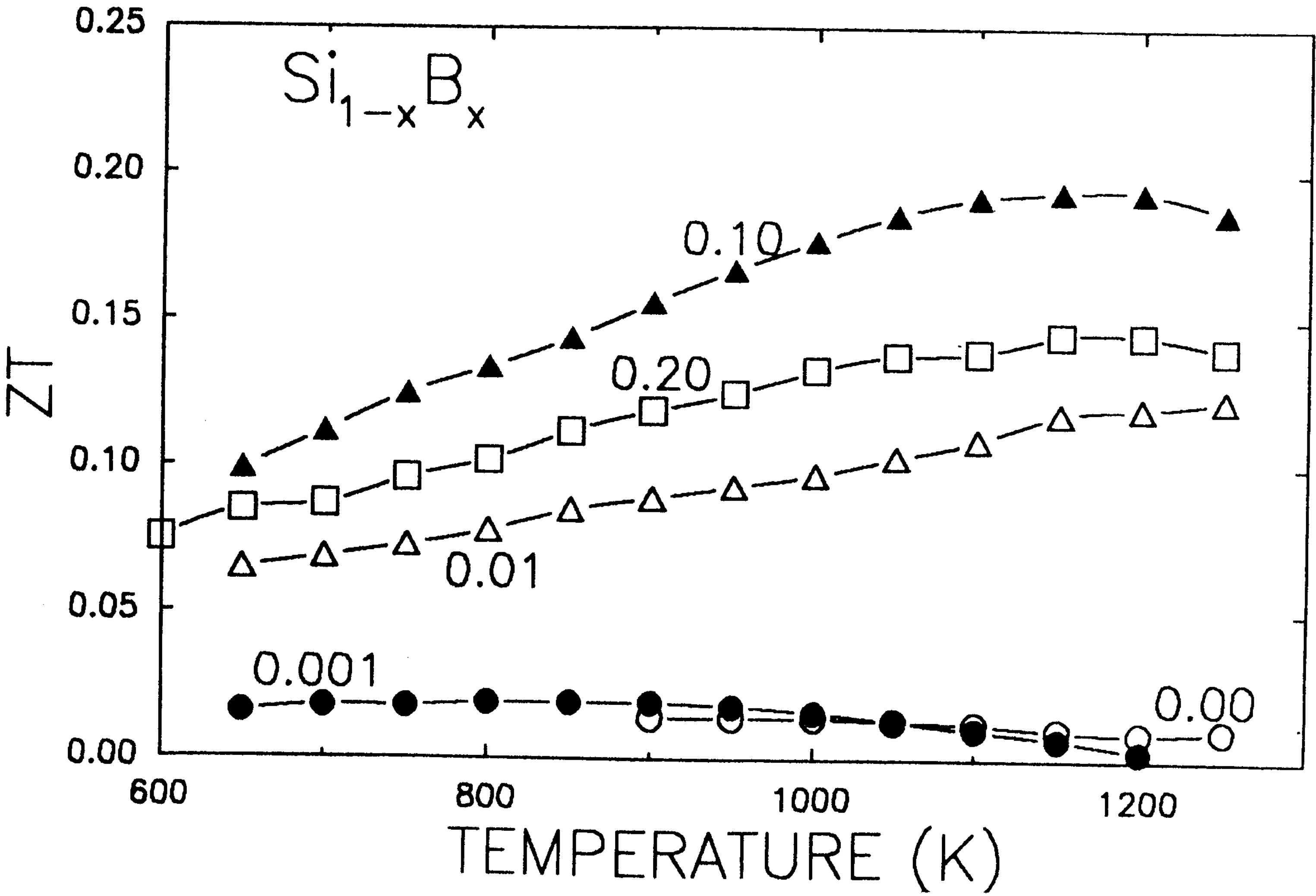

Figure 13: The dimensionless figure of merit ($S^2T/\rho\lambda$) as a function of temperature for four samples of boron-doped silicon and one sample of undoped silicon. The undoped silicon sample is n-type, while the four boron-doped samples are p-type.

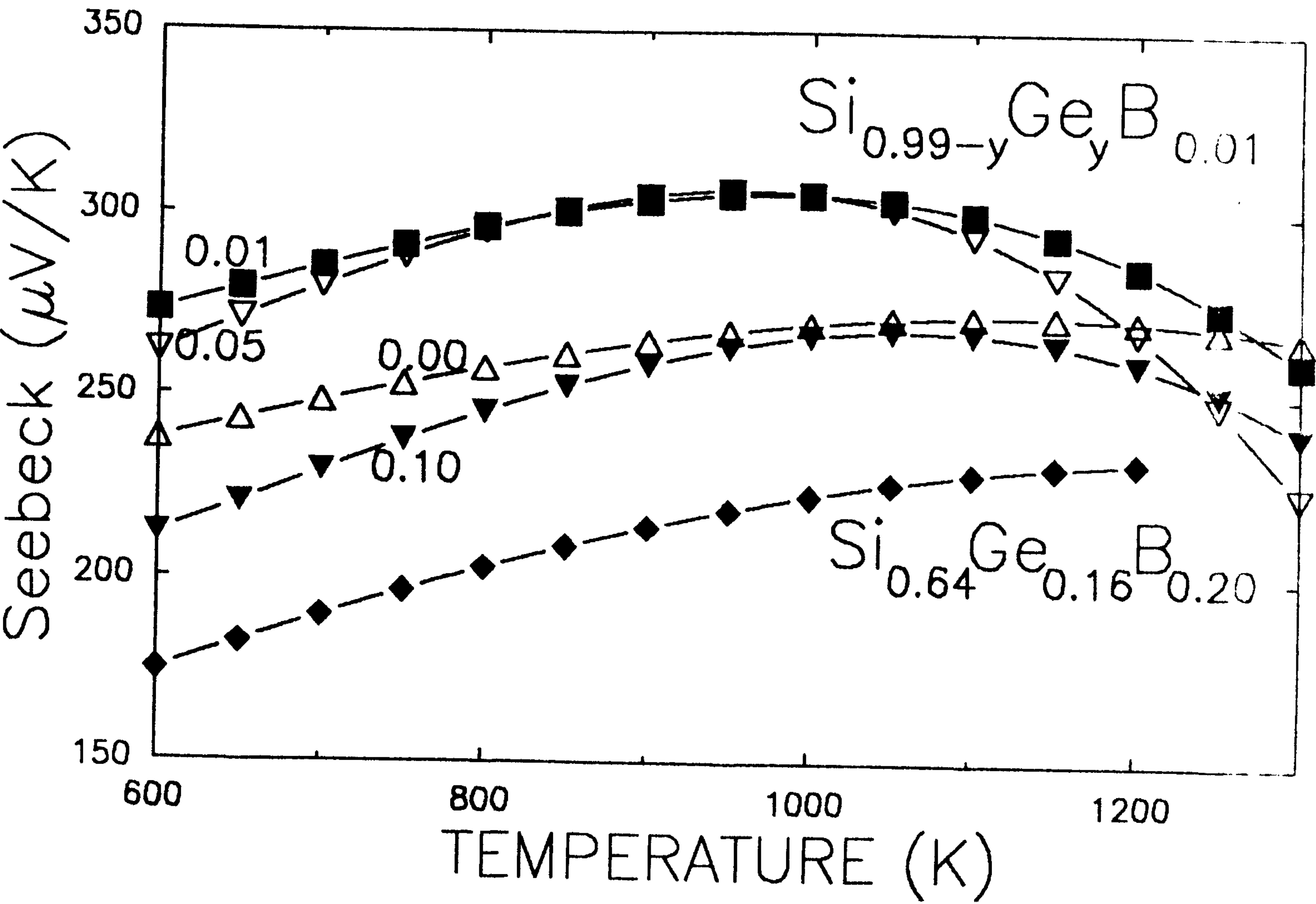

Figure 14: The Seebeck Coefficient as a function of temperature for five samples of boron-doped silicon-germanium.

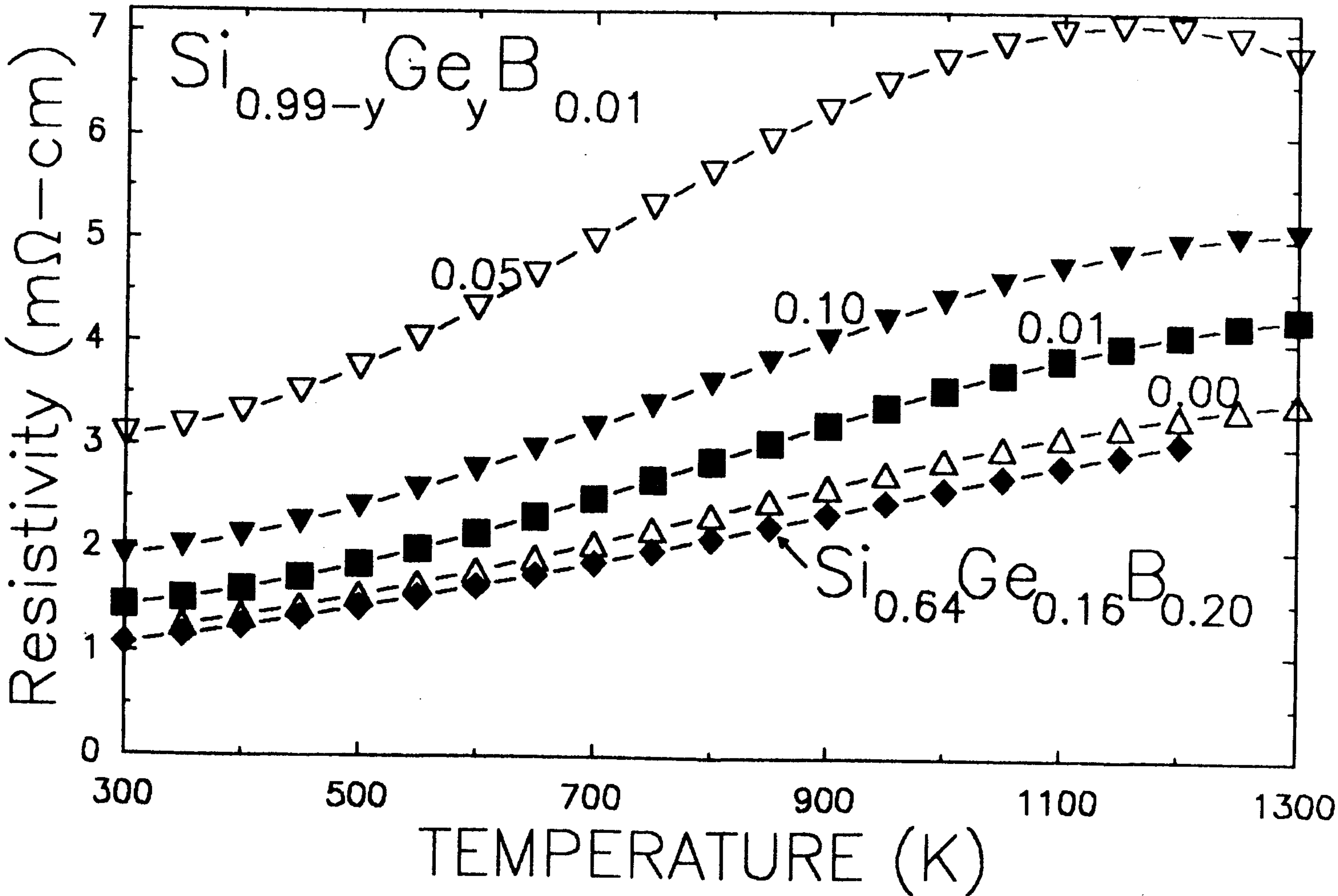

Figure 15: The electrical resistivity as a function of temperature for five samples of boron-doped silicon-germanium.

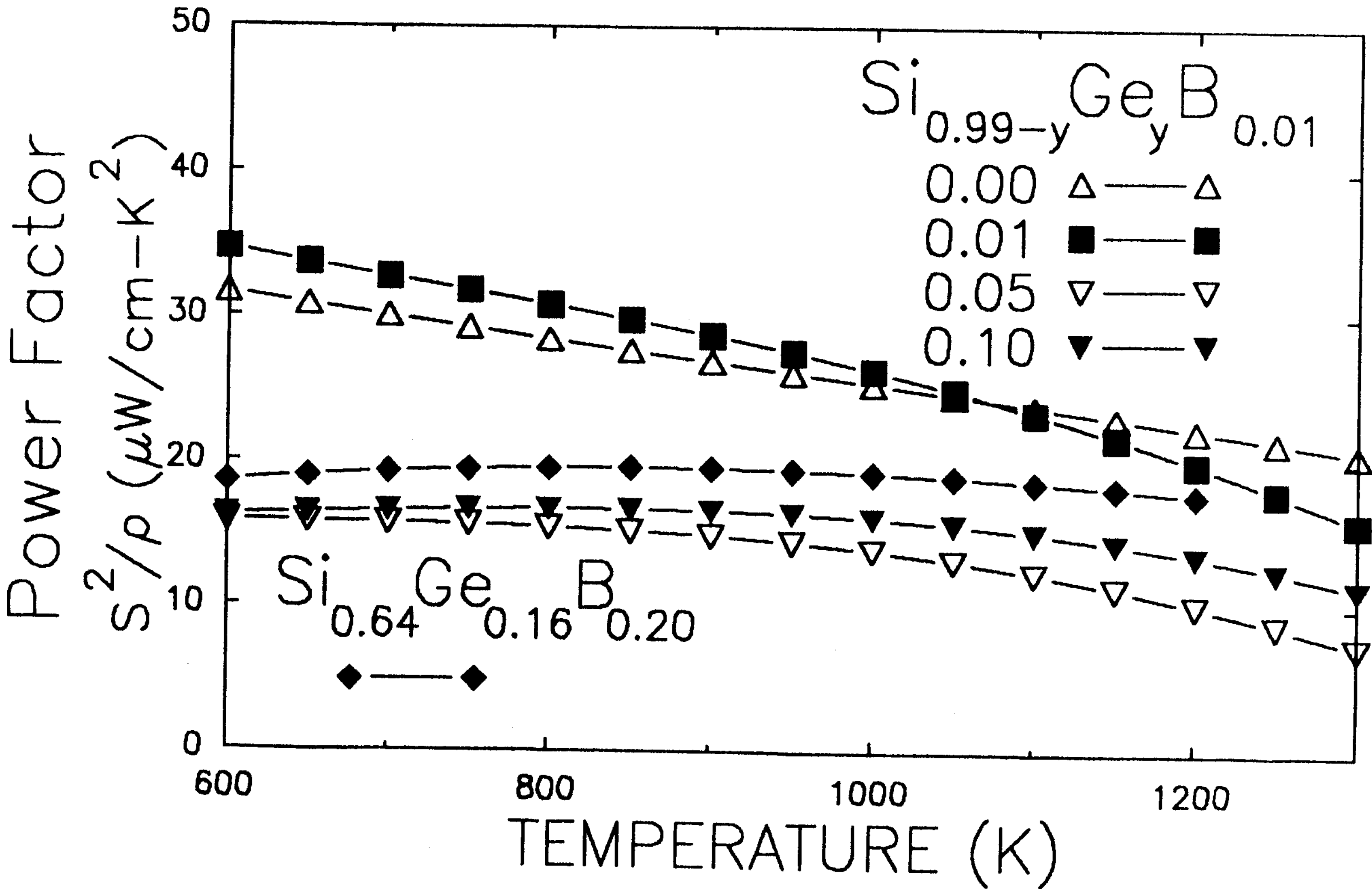

Figure 16: The electrical power factor (S^2/ρ) as a function of temperature for five samples of boron-doped silicon-germanium.

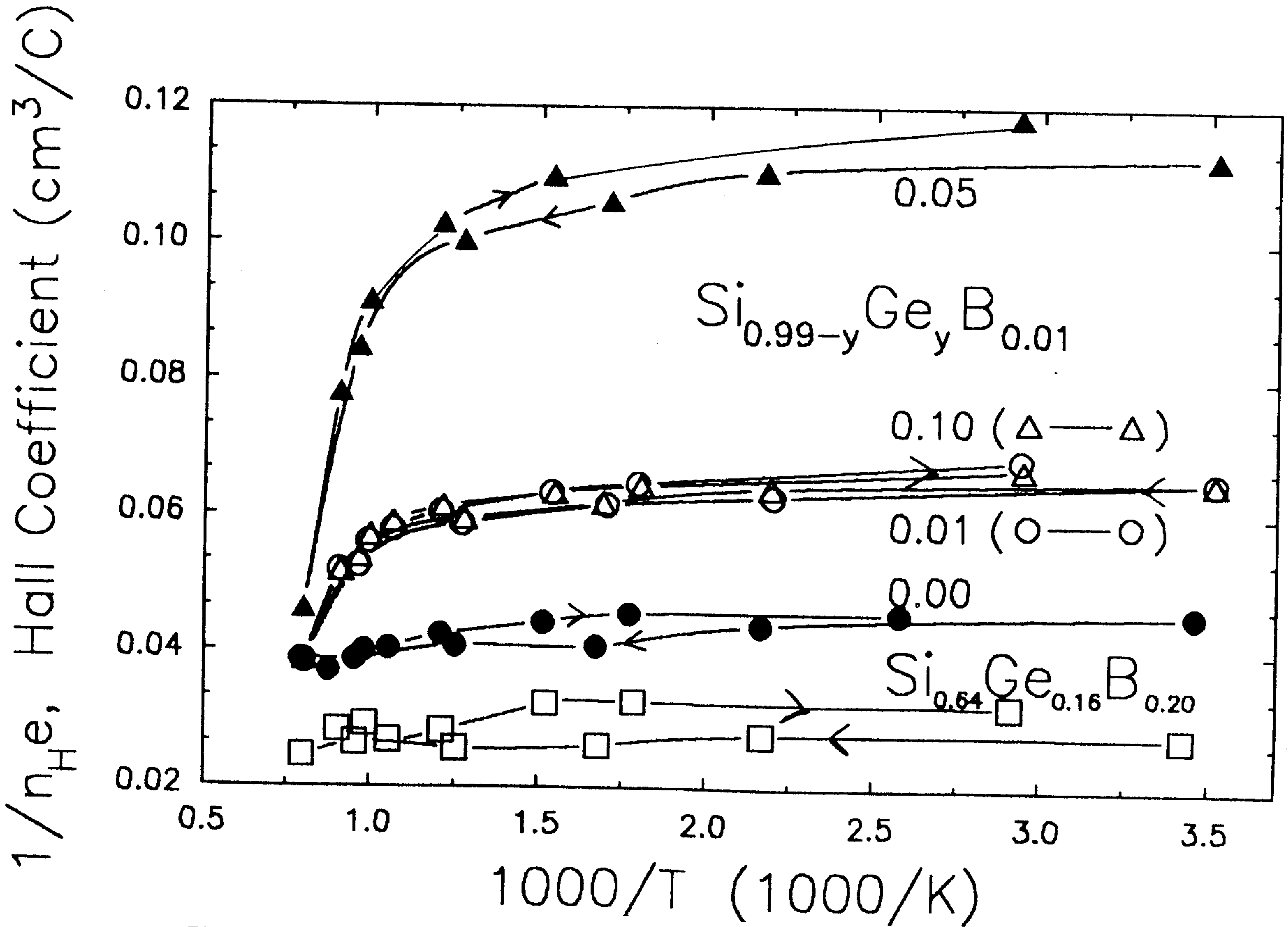

Figure 17: The Hall coefficient (1/ne) as a function of inverse temperature for five samples of boron-doped silicon-germanium. The left and right arrows indicate data collected while the sample temperature was increasing and decreasing, respectively. Note that the Hall coefficient higher (carrier concentration lower) during cooling compared to the warming data.

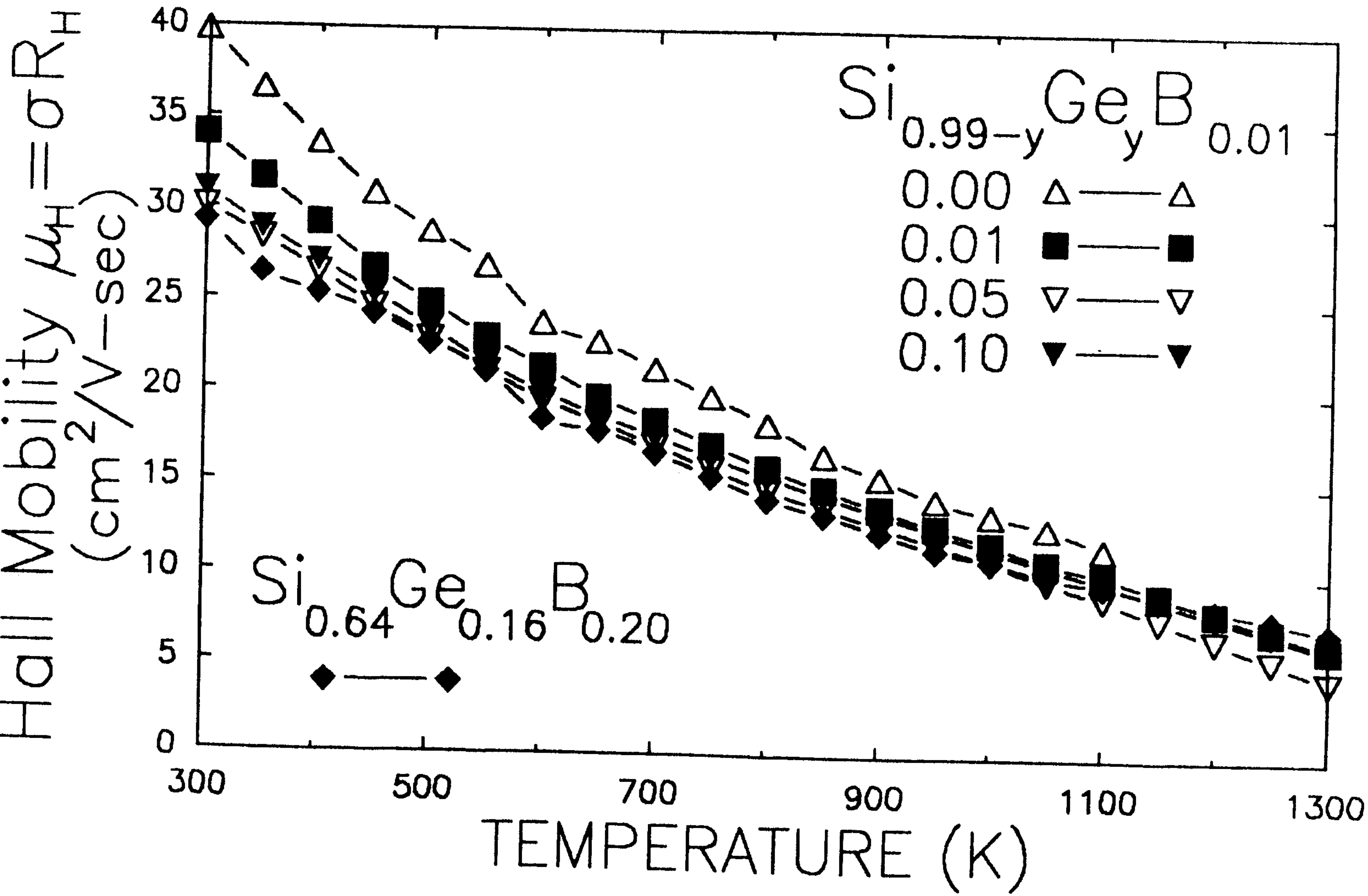

Figure 18: The Hall mobility as a function of temperature for five samples of boron-doped silicon-germanium. Note that the mobility generally decreases as the germanium content increases.

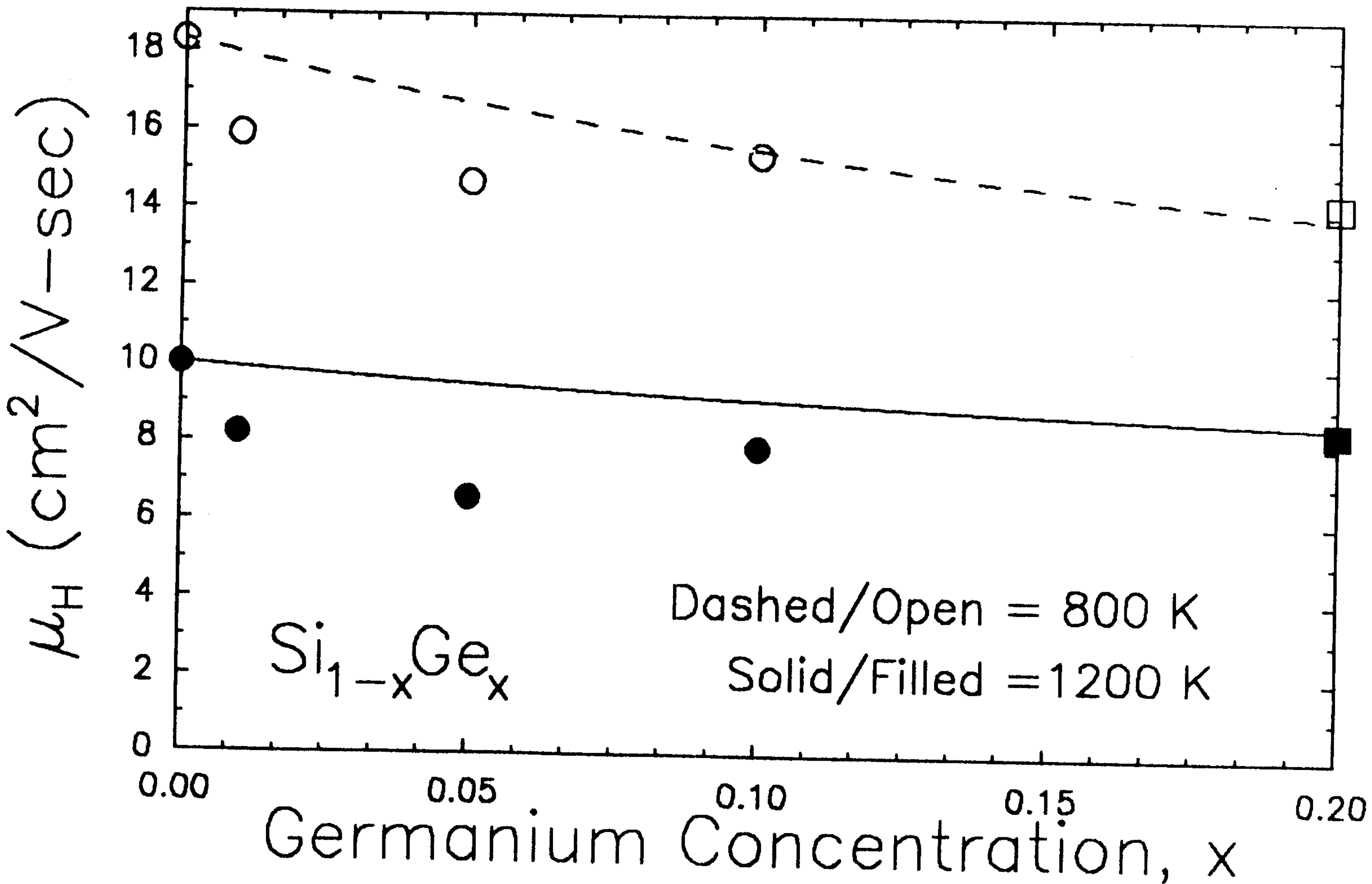

Figure 19: The Hall mobility as a function of germanium content for five samples of boron-doped silicon-germanium at 800 K and 1200 K. The mobility generally decreases as the germanium content increases, but the agreement with simple theory, given by the lines, is qualitatively poor.

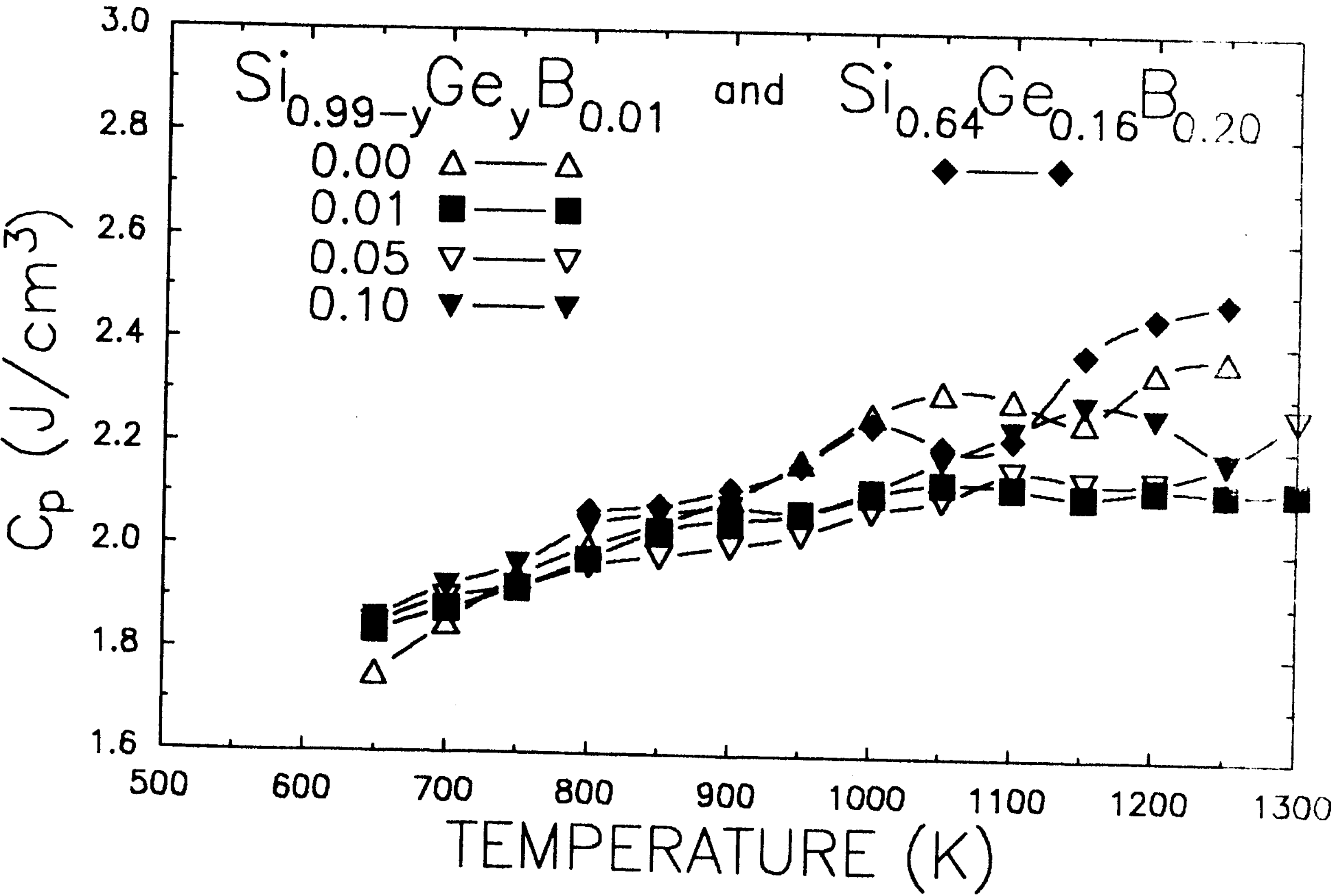

Figure 20: The heat capacity of five samples of boron-doped silicon-germanium. The somewhat larger variation in heat capacities observed at the highest temperatures is attributed to experimental uncertainties, but represents only modest absolute errors for this type of measurement.

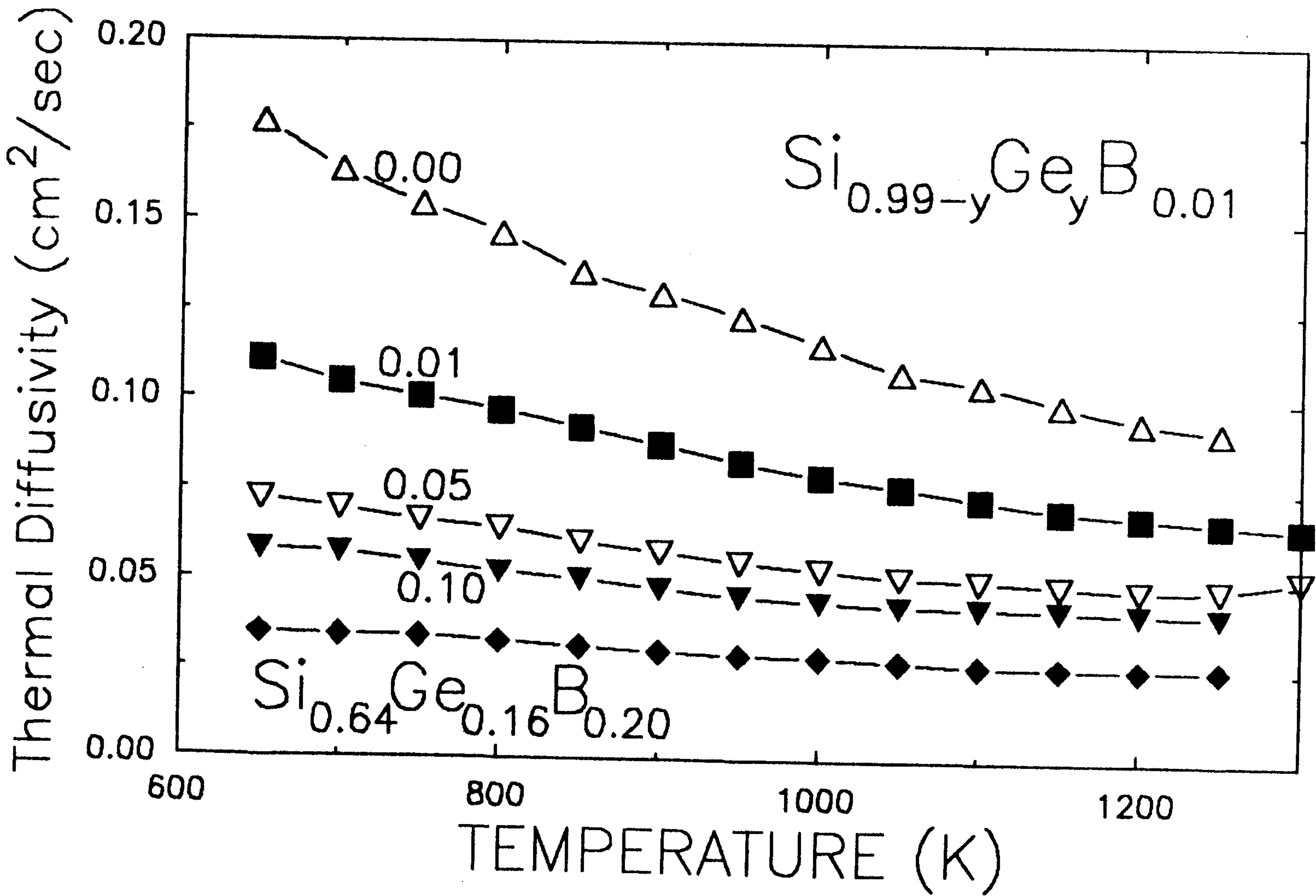

Figure 21: The thermal diffusivity as a function of temperature for five samples of boron-doped silicon-germanium. The thermal diffusivity decreases with increasing germanium content.

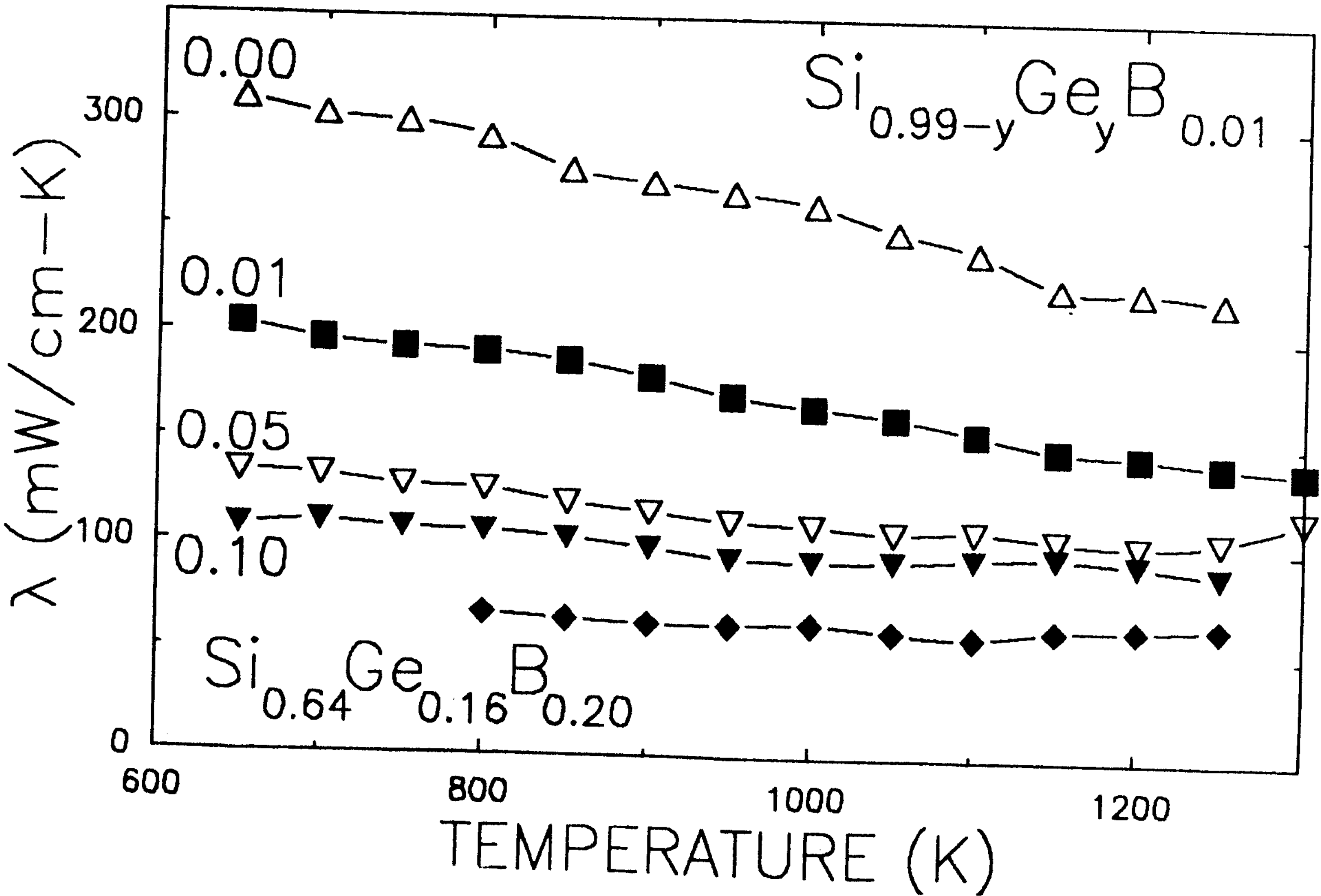

Figure 22: The thermal conductivity as a function of temperature for five samples of boron-doped silicon-germanium. The thermal conductivity decreases with increasing germanium content.

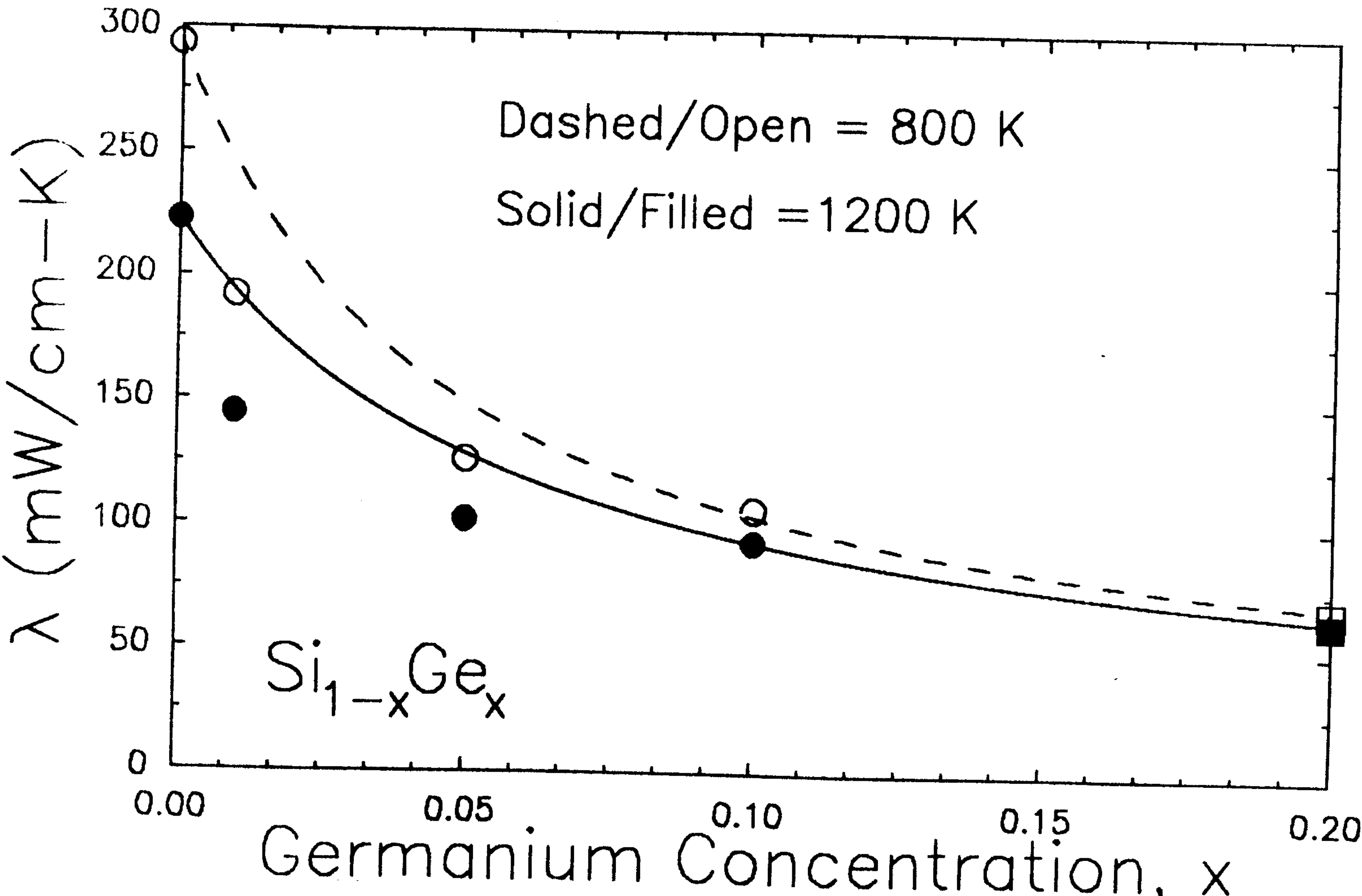

Figure 23: The thermal conductivity as a function of germanium content for five samples of boron-doped silicon-germanium at 800 K and 1200 K. The thermal conductivity generally decreases as the germanium content increases, but the agreement with simple theory, given by the lines, is qualitatively poor.

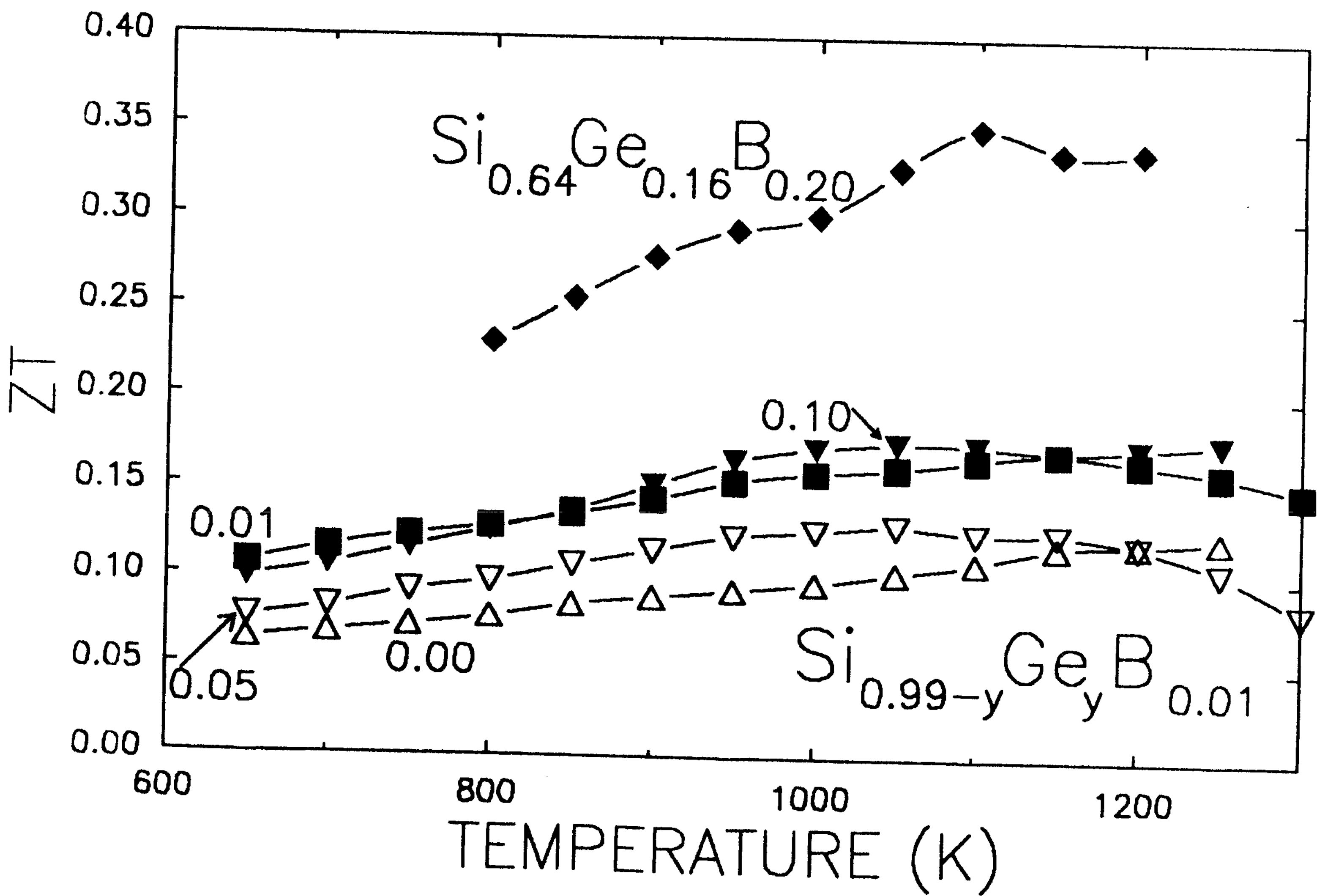

Figure 24: The dimensionless figure of merit ($S^2T/\rho\lambda$) as a function of temperature for five samples of boron-doped silicon-germanium.